CHAPTER 8: STUDY OF GROUND IMPROVEMENT FOR A STUB ABUTMENT

8.1 Overview

The effectiveness of ground improvement for mitigating the effects of liquefaction on the stub abutment of a bridge was investigated to complement the study conducted for a pier on a shallow foundation. A fundamental difference between a pier and a stub abutment supported on an approach embankment is the presence in the abutment case of a net shear force in the ground acting in the longitudinal direction of the bridge towards the center. Therefore, the remediation scheme for the stub abutment must be able to resist the tendency for lateral spreading during earthquake shaking and liquefaction of the unimproved soils, which can produce large horizontal movements in addition to large vertical movements.

Similar to the analyses conducted for the pier described in the previous chapter, the main focus of the parametric study for the stub abutment was the effect of the type, properties, size, and location of the ground improvement on the predicted permanent displacements of the abutment. In particular, an effort was made to establish whether ground improvement could be used to reduce the predicted movements of a stub abutment to levels tolerable for a bridge. Like the pier case, the analyses were performed using the Pyke-Byrne soil model implemented in FLAC.

The parametric study for the stub abutment focused on ground improvement methods that were qualitatively judged to have moderate to high applicability for remediation at such an abutment, as discussed in Chapter 2, Section 2.2. Only one abutment and soil profile subjected to one earthquake motion were used in the analyses, so broad generalizations regarding the use of ground improvement at abutments are not possible. However, the results of the analyses provide insights regarding the effectiveness of different ground improvement types and configurations for mitigating potential damage in this particular case, as well as similar cases. General details regarding the stub abutment case analyzed and boundary conditions used are presented below. This information is followed by a discussion of the ground improvement

configurations analyzed and the results obtained. The implications of the results concerning the use of different ground improvement types for liquefaction remediation at a stub abutment are then summarized.

As discussed in Chapter 7, Section 7.1, the movement criteria given in Chapter 4, Section 4.2.1, were used as a guide for establishing tolerable movements for the test problem bridge. Like the bridge pier case, an upper limit of acceptable displacement of 10 centimeters was used for both the horizontal and vertical movements of the stub abutment. Based on the observations of predicted versus measured movements in the verification analyses performed (refer to Chapter 6, Section 6.4), predicted vertical and horizontal displacements of 5 cm were set as the approximate upper bounds of tolerable predicted movement.

8.2 Case Evaluated

The stub abutment and soil profile used in the parametric study are from the test problem in Chapter 5, Section 5.4.1. More details are given below regarding the abutment, soil properties, earthquake motion, ground improvement types, finite difference grid, and two-dimensional simplifications used in the analyses.

8.2.1 Stub Abutment Configuration and Loads

The stub abutment consists of a L-shaped beam seat constructed of reinforced concrete and supported on a spread footing at the top of an approach embankment constructed of dense, well-graded gravelly sand, as shown in Chapter 5, Figures 5.35 and 5.36. In the FLAC analyses the stub abutment was represented in the finite difference grid by a group of elements that were assumed to be elastic material with high shear and bulk moduli similar to concrete, as shown in Figure 8.1. To simplify the analysis, no interface elements were used between the abutment elements and the soil elements representing the embankment.

Preliminary FLAC analyses were performed for the stub abutment where the superstructure load acting on the abutment was modeled as a concentrated point load, which simulates roller bearings at the end of the superstructure beams. As an alternative approach the superstructure was also modeled as a structural member pinned to the abutment. The predicted movements for the abutment using the point load representation of the superstructure were larger

than those obtained using the pinned structural member. Therefore the parametric study analyses were performed using a concentrated point load of 100 kilonewtons per meter (kN/m) to represent the superstructure load on the abutment in a two-dimensional analysis, as shown in Figure 8.1.

In the preliminary FLAC analyses some tilting of the abutment occurred during the earthquake shaking simulation, resulting in slightly different vertical movements being predicted at different points on the abutment. However, for the purposes of evaluating the performance of the stub abutment the movement predicted at the concentrated point load was used because that location was near the middle of the beam seat for the superstructure.

In addition to variations in vertical movement across the abutment, there were some differences between the horizontal movement predicted for the abutment and the horizontal movements predicted in the lower part of the embankment and underlying foundation soils. The horizontal movements predicted in the underlying embankment and the foundation soils were as much as 30 to 50 percent greater than at the abutment. This larger horizontal movement can probably be attributed to the settlement of the embankment into the underlying soils which has the tendency to push those soils outward from the embankment. Since the trends in the abutment movements with variations in assumed conditions appeared reasonable and the performance of the bridge is more dependent on the abutment displacements than on the underlying soil movements, the horizontal movement of the abutment at the point load was used for performance evaluation and comparison purposes.

8.2.2 Soil Profile

The soil profile and properties beneath the stub abutment and approach embankment were the same as those used for the pier. A schematic of the soil profile is shown in Chapter 5, Figure 5.35. Properties and parameters for the soil strata underlying the approach embankment are given in Table 7.2. The property and parameter values used for the dense gravelly sand embankment itself are given in Table 8.1.

8.2.3 Earthquake Motion

The performance of the abutment was evaluated for the same scaled record of motion from the Kobe earthquake used in the pier study. Details concerning this motion can be found in Section 7.2.3. The acceleration, velocity, and displacement time histories for the motion are

shown in Figure 7.4. Like the pier analyses, the velocity record was used as the dynamic input for the FLAC analyses of the stub abutment.

8.2.4 Ground Improvement Types and Factors

Several different improved ground types were evaluated for mitigating the effects of liquefaction on the stub abutment and supporting approach embankment including:

- No improvement;
- Densified zone of limited size beneath and around the approach embankment created using compaction grouting;
- Chemically-grouted zone beneath and around the embankment;
- Jet-grouted zone under the approach embankment slope; and
- Buttress fill placed against the slope.

A schematic illustrating the use of a densified, chemically-grouted, or jet-grouted zone at a stub abutment and supporting approach embankment is presented in Figure 2.8. Use of a buttress fill for remediation is illustrated in Figure 2.10.

Like the parametric study performed for the pier, the treatment factors investigated for different remediation methods at the stub abutment included the properties, size, and/or location of the improved zone. The particular factors investigated for a specific improvement type are discussed below in the section pertaining to that treatment method, along with the results of the FLAC analyses.

8.2.5 Grid and Boundary Conditions

A schematic is presented in Figure 8.2 of the finite difference grid used in the FLAC analyses of the stub abutment and approach embankment. As seen from this figure, the vertical boundaries of the grid were placed a distance approximately five times the soil layer thickness away from the stub abutment to limit the effects of the side boundary proximity on the predicted performance of the abutment. The gradation of the grid was selected so that further refinement would not result in a significant change in the predicted abutment response.

The finite difference grid in Figure 8.2 shows a small vertical face along the slope of the approach embankment in front of the stub abutment. This face does not exist in the actual test

problem, but resulted from the sequence of commands given in FLAC to form the sloping embankment and stub abutment within the grid. The two elements immediately adjacent to this face were assigned a cohesion of 24 kPa to prevent them from distorting excessively and causing difficulties with the FLAC runs.

Simulation of earthquake shaking in the dynamic analyses was accomplished by applying the horizontal velocity record in Figure 7.4 to nodes at the vertical side boundaries and base of the grid shown in Figure 8.2. Nodes at the base of the grid were fixed against movements in the vertical (y) direction. The application of the earthquake motion to embankment nodes along the left side of the grid simulates a condition where the embankment comes into direct contact with non-liquefiable soils at a distance of approximately 75 meters behind the abutment due to an end of the liquefiable soil layers.

Pore water pressures were fixed to 0 kPa at the top of the liquefiable soils (liquefiable soils include the 3-m-thick medium dense sand layer and underlying 8-m-thick loose sand layer shown in Figure 5.35) outside the embankment to simulate a free-draining surface. In addition, pore water pressures were fixed to 0 kPa at the top of the liquefiable soils under the embankment to avoid the complication of modeling partially saturated flow into the embankment. Some preliminary analyses performed where the pore water pressures were not fixed to 0 kPa at the top of these soils under the embankment gave predicted embankment deformations similar to those obtained when it was fixed. Therefore the simplification of fixing the pressures appeared reasonable.

Predicted ground responses in the immediate vicinity of the stub abutment during dynamic loading were of particular concern in the analyses performed. The finite difference grid in this area is shown at a larger scale in Figure 8.3. Some locations where ground and abutment responses were obtained, as discussed later, are indicated in the figure.

8.2.6 2-Dimensional versus 3-Dimensional

As seen from the finite difference grid in Figure 8.2, two-dimensional (2-D) analyses were performed of the stub abutment when the test problem shown in Figure 5.36 is actually three-dimensional (3-D). Like the pier analyses, no attempts were made to adjust the 2-D results for 3-D effects. Excess pore water pressures in treated zones were not adjusted for 3-D pore pressure migration effects. Additional research would be required to make such adjustments, including performing 3-D analyses for comparison with the 2-D analyses. Although the

magnitudes of the predicted response might vary somewhat between 2- and 3-D analyses for the test problem evaluated, many of the trends seen in the 2-D analyses would likely be seen in the 3-D analyses. The difference between 2-D and 3-D analysis results would be expected to diminish as the width of the bridge and stub abutment increases, provided the unit loading conditions remain the same.

8.3 No Improvement

8.3.1 Observed Behavior

An analysis was performed of the stub abutment and approach embankment supported on the liquefiable soils without ground improvement to see if the predicted permanent movements caused by the simulated earthquake shaking were excessive. In the event the movements were unacceptable, this case would serve as a basis for judging the effectiveness of different ground improvement methods and configurations for mitigating the effects of liquefaction on the abutment performance, particularly the induced permanent displacements.

A limited number of vectors representing the displacements predicted in the vicinity of the stub abutment for the case of no improvement are shown in Figure 8.4. Each vector indicates the magnitude and direction of the displacement predicted for the nodal point located at its tail. The magnitude of the vectors range from 75 to 110 cm, with the exception of the lowest row where the displacement ranges from 23 to 57 cm. The vectors indicate that the predominant movement is in the horizontal direction with an orientation toward the lower elevation area in front of the embankment. The vertical component of movement is smaller, acting in a downward direction under the abutment and upward at the embankment toe.

Time histories of the predicted vertical (y) and horizontal (x) movements of the abutment for the no improvement case are presented in Figures 8.5 and 8.6. As seen from Figure 8.5, the predicted horizontal displacement of Point D1 on the abutment relative to the grid base increased significantly in the positive x-direction (see Figures 8.3 and 8.4 for direction) between 4 and 10 seconds, reaching a final value of approximately 82 cm. Likewise, the predicted settlement (corresponds to a vertical displacement in the negative y-direction) of the abutment at D1

increased to a final value of about 32 cm from 4 to 13 seconds, at which time the strong shaking ended and the settlement was relatively unchanged.

Unlike the predicted horizontal movement of the bridge pier footing relative to the grid base during shaking, the movement of the abutment relative to the base is generally only in the positive x-direction. This movement is confirmed by the x-velocity records for these two locations shown in Figure 8.7. As seen from this figure the abutment and base have similarly increasing positive x-velocities, but the positive velocity peaks of the abutment are larger. In addition, the negative velocity peaks of the abutment are much lower (closer to zero) than the base. This behavior results in the net positive x-displacement of the abutment relative to the base. It indicates that the abutment has a tendency not to follow the base as the base reverses its direction of horizontal movement from positive to negative, except during the very early and late stages of the strong motion.

The tendency for the abutment to move with the base in the positive x-direction, but not the negative, throughout a large portion of the strong motion can be explained by the development of positive excess pore water pressures under the embankment and the boundary conditions. As shown in Figures 8.8 and 8.9, significant excess pore water pressures start developing under the embankment at a time of about 4 seconds. The excess pore water pressure ratios of 0.6 to 0.9 that develop at depths of about 5 meters and more below the top of the liquefiable soils under the embankment are sufficient to cause significant softening and strength loss in the soil. As a result of this softening and loss of strength the lower liquefiable soils undergo large deformations when subjected to shear stress. When the base moves in the positive x-direction the abutment follows the base largely because the stiff embankment and upper liquefiable soils that develop lower excess pore pressures are being pushed by the side of the grid where the input motion is also being applied. Therefore, for movement in the positive x-direction the base motion does not have to be transmitted to the abutment through the lower liquefiable soils that have lost considerable strength and stiffness. Movement in the negative x-direction applied to the grid sides can not be transmitted directly by the embankment and upper liquefiable soils to the abutment because the sides of the grid would in essence be trying to pull these soils, which have no tensile strength. Therefore, the movement of the abutment with the base in the negative x-direction would require the development of relatively high shear stresses in the liquefiable soils. However, the lower liquefiable soils have low strength due to high

excess pore water pressures, resulting in large shear deformations in this zone and movement of the base without the abutment.

The excess pore pressure ratio time histories in Figures 8.8 and 8.9 indicate that the deeper liquefiable soils under the embankment are closer to liquefaction than the shallow soils. The lower pore water pressures at shallow depth are probably due to a combination of the higher relative density of the medium dense sand layer compared to the underlying loose sand layer and movement of the medium dense layer with the stiff, dense embankment. These factors appear to result in larger shear deformations in the deeper loose sand. The time histories of excess pore pressure ratios at points P7, P8, and P9 in the free-field presented in Figure 8.10 indicate that nearly all of the soils in the free-field liquefy, as indicated by the r_u values of 1.0.

8.3.2 Implications

Excessive permanent displacements are predicted for the stub abutment and approach embankment due to liquefaction of the underlying sands during the simulated earthquake motion. Therefore, remediation measures, such as ground improvement, are necessary to mitigate liquefaction and reduce abutment movements to levels that are less likely to cause bridge damage. The effectiveness of different ground improvement measures for this purpose are discussed in the remaining sections of this chapter.

8.4 Densification

8.4.1 Properties and Factors

Densification of the liquefiable soils beneath the stub abutment and approach embankment using compaction grouting was considered as a potential remediation method in the parametric study. The effects of the degree of densification, width, and location of the densified zone on the predicted performance of the stub abutment were investigated. The densified zone was assumed to extend from the bottom of the embankment to the bottom of the liquefiable soils in all of the cases evaluated. Figure 5.39(a) presents a general illustration of the 2-dimensional problem analyzed in FLAC.

In evaluating the densified zones for liquefaction remediation at the stub abutment, the properties assumed for the densified sand were the same as those used for the pier case described

in Section 7.4.1. Densification of the liquefiable sands to a relative density of 75 or 85 percent was assumed. The presence and effects of the compaction grout columns themselves on performance were ignored. Properties used for the densified zones in the analyses were the same as those presented in Table 7.3.

8.4.2 Effects on Response and Performance

8.4.2.1 General

One of the cases analyzed for densification improvement at the stub abutment consisted of a zone densified to 85 percent relative density and extending continuously in the lateral direction from 19 meters behind the embankment crest (i.e. – behind the back of the stub abutment) to 8 meters in front of the embankment toe, with the total zone width being 39 meters. The location of this densified zone relative to the stub abutment is shown in Figure 8.3. As previously mentioned the densified zone extended completely through the liquefiable soils from the bottom of the embankment to the bottom of the liquefiable soils.

Time histories of the predicted horizontal (relative to the grid base) and vertical (y) displacements of the abutment during shaking are presented in Figures 8.11 and 8.12. As seen from these figures the presence of the densified zone dramatically reduces the predicted displacement of the stub abutment compared to the no improvement case. The final horizontal (x) movement of the abutment is approximately 7.6 cm and the final settlement is about 4.5 cm.

The plot in Figure 8.11 indicates the abutment more or less moved together with the base of the grid in the horizontal direction up until a time of about 7 seconds, when the horizontal displacement of the abutment relative to the base became progressively larger in the positive x-direction. The tendency of the abutment to move together with the base in both directions is further confirmed by Figure 8.13 where the time histories of x-velocity for the base and Point V1 on the abutment are shown together. Unlike the no improvement case, the trends in the x-velocity of the abutment are similar to those of the base, with the abutment having somewhat higher peaks, particularly in the positive direction. Thus the presence of the densified zone allowed the abutment to follow the base more closely than for the case of no treatment, resulting in a smaller net horizontal displacement at the end of shaking.

The ability of the densified zone to reduce the predicted vertical and horizontal displacements of the abutment can be attributed to the higher strength and relatively stiff

behavior of the densified zone. The stiff behavior was implemented in the analysis by assuming a higher shear modulus for the densified soil than the unimproved soil, as well as modifying the volumetric strain constants C_1 and C_2 so less volumetric strain developed during cyclic shear loading. The reduction in the induced volumetric strain is evident by the lower predicted excess pore pressure ratios for Points P4, P5, and P6 in the dense zone shown in Figure 8.14 compared to the excess pore pressure ratios for the same locations in the no improvement case shown in Figure 8.9. The reduction in the excess pore water pressure ratio was particularly evident at greater depths below the embankment, such as Point P4 where the peak ratio was reduced from about 0.6 to 0.3. An excess pore water pressure ratio greater than 0.5 results in significant softening of liquefiable soil, which explains the large deformations for the no improvement case and the reduced movements seen when the ratio dropped to 0.3 for the densified zone case.

Although the excess pore water pressure ratio was reduced in the zone that was densified, there was no reduction in the excess pore pressure ratio in the unimproved soils remaining under the embankment. This is evident from a comparison of the time histories of excess pore water pressure ratios at Points P1, P2, and P3 for the densified zone case presented in Figure 8.15 and the unimproved case presented in Figure 8.8. Therefore, it appears the densified zone prevented large shear deformations from occurring in the unimproved soils under the embankment, which still developed high excess pore pressures, by restraining lateral movement of these soils.

The results presented for this case indicate that the movement of a stub abutment located over liquefiable soils can be reduced by densifying a zone in the liquefiable soils under the approach embankment supporting the abutment. However, the magnitude of the reduction achieved is dependent on the relative density, width, and location of the improved zone.

8.4.2.2 Location, Width, and Degree of Densification

A parametric study was conducted to investigate the effect of the location, width, and relative density of the densified zone on the predicted performance of the stub abutment supported on the approach embankment. The analyses were divided into four separate groups with the purpose of systematically identifying the properties and configuration of a densified zone that effectively reduced the predicted movements of the stub abutment to a tolerable range. In each of the groups different cases were evaluated involving variations in the location, width, and/or relative density of the treated zone. The cases analyzed and their groupings are shown in

Figure 8.16. A summary is given in Table 8.2 of the relative densities, widths, and locations assumed for the densified zones for each case within a respective group.

In the Group 1 analyses, the emphasis was placed on establishing the extremes in performance that could be obtained for zones densified to 75 percent relative density and having widely different locations and sizes. The first analysis in this group (Case A) consisted of a densified zone extending from the crest (i.e. – back of the abutment) to toe of the embankment. This case was based on the finding by Riemer et al. (1996), from numerical analyses, that a treated zone was generally most effective in reducing the deformations of an embankment when centered under the slope of the embankment (refer to Chapter 3, Section 3.2.1.1). The remaining analyses in the group consisted of extending the densified zone under the slope to either end of the grid, as well as treating all of the liquefiable soils underneath and outside the embankment.

Figure 8.17 presents a graphical summary of the predicted movements of the stub abutment at point D1 for the different treatment cases in Group 1. Numerical values for the predicted displacements are given in Table 8.2. As seen from Figure 8.17 and Table 8.2, none of the densified zone cases in Group 1 were able to reduce the predicted vertical and lateral movements of the stub abutment to the range of about 5 cm, with the exception of treating all of the liquefiable soils underneath and outside the embankment (Case D). Treating all of the liquefiable soils gave predicted horizontal and vertical abutment displacements of 6.8 and 6.5 cm, respectively.

Treating the liquefiable soils under the slope and either all of the liquefiable soils outside (Case B) or underneath (Case C) the embankment did not reduce the abutment movements to tolerable levels. The predicted displacement vectors shown in Figures 8.18 and 8.19 for these two cases clearly show that the abutment and ground movements were reduced and the pattern of movements modified compared to the no improvement case (Figure 8.4). However, in Case B there was too much lateral displacement of the ground under the embankment slope towards the free-field. In Case C there was excessive downward and outward movement of the slope toward the free-field indicative of a localized shear zone near the slope. Short of treating all of the liquefiable soils, the overall results seemed to indicate some combination of treating the liquefiable soils a limited distance in front of the toe and behind the crest would be necessary to reduce the abutment movements to an acceptable range.

The Group 2 and Group 3 analyses focused on establishing a combination of densification under and outside the embankment that resulted in tolerable movements. In the Group 2 analyses the cases evaluated included a densified zone at 75 percent relative density under the embankment slope and extending in front of the embankment toe varying distances. As seen from Figure 8.20, significant reductions in predicted horizontal and vertical movements of the abutment were obtained by extending the treated zone out beyond the toe a distance of approximately 8 meters (Case F). Although further reductions were obtained for zones extending even more than 8 meters beyond the toe, the magnitude of the reduction with increasing distance was progressively lower. Therefore, the 8-meter distance was selected as striking a balance between limiting the densified zone size and limiting the abutment displacements.

With the boundary for the densified zone outside the embankment slope fixed at 8 meters beyond the toe, analyses were performed in Group 3 to establish an appropriate location for the other boundary behind the crest. These cases included extending the zone at 75 percent relative density to distances of 19 and 39 meters behind the crest. A plot of the predicted vertical and horizontal movements of the abutment versus the treatment distance behind the crest is presented in Figure 8.21. The results of the analyses indicate that a treatment distance of 39 meters behind the crest, giving a total width of 59 meters (Case I), brings the predicted abutment movements down close to the tolerable range for bridges given in Table 4.1. The predicted horizontal and vertical movements of 7 and 8 cm, respectively, are close to the lower limit of displacements obtained when all of the liquefiable soils (i.e.- both under and outside the embankment) are treated to 75 percent relative density.

Given the large treated zone size required for tolerable abutment displacements when a section of the liquefiable sands is improved to 75 percent relative density, two analyses were performed (Group 4) assuming a relative density of 85 percent. In these analyses the densified zone limits extended from 8 meters in front of the embankment toe to 19 and 29 meters behind the crest (Cases J and K). The variation of the predicted abutment displacements with the treatment distance behind the crest is shown in Figure 8.22, along with the limiting displacements obtained assuming all of the liquefiable soils (underneath and outside of the embankment) were densified to 85 percent. As seen from this figure, there does not appear to be a substantial difference in the predicted results for the two cases. The predicted horizontal and

vertical abutment displacements for the 19-meter-distance case (total treatment width of 39 meters) are 7 and 4.5 centimeters, respectively, and for the 29-meter-distance case (total width of 49 meters) they are 6 and 7.1 centimeters. However, it should be noted that both smaller horizontal and vertical movements were predicted for the 29-meter case (final values of 4 and 5 cm, respectively) when the accumulated volumetric strain parameter (used in the Byrne volumetric strain formula for the pore water pressure generation code) for each element was initialized back to zero from a value of 10^{-6} to 10^{-7}. This initialization was performed after establishing the initial stress state and switching to the Pyke-Byrne model, but before applying the dynamic loading.

Displacement vectors at the end of shaking are shown in Figure 8.23 for the zone densified to 85 percent relative density and extending 19 meters behind the crest (Case J). The vectors are similar in terms of direction to those appearing in Figure 8.18 for treatment from the crest of the embankment to the right end of the grid. However, the magnitudes of the vectors in Figure 8.23 are less than 30 percent of the magnitudes shown in Figure 8.18, and less than 50 percent of the magnitudes in Figure 8.19.

Based on the analyses performed in this parametric study, it appears the horizontal and vertical abutment movements for the test problem could be reduced to tolerable levels using a zone densified to 85 percent relative density and having a width in the range of 39 to 49 meters. The zone would extend continuously from a boundary located somewhere between 19 and 29 meters behind the embankment crest to another one located 8 meters beyond the toe. The predicted displacements for the treatment width of 39 meters are on the borderline of being acceptable based on the upper limit of 5 cm for tolerable predicted vertical and horizontal displacements discussed in Section 8.1. However, Youd et al. (1998) notes that some newer bridges have survived up to 20 cm of lateral ground movement, making the 39-meter-width of treatment potentially viable depending on the level of performance required for the bridge.

8.4.2.3 Excess Pore Water Pressure Migration

All of the analysis results presented above for the stub abutment supported on a densified zone were for time durations of 26 seconds, which was approximately 13 seconds beyond the end of strong shaking in the simulated earthquake record. However, there is potential for excess pore water pressure migration to occur from untreated zones having high excess pore water pressures to the densified zone having low excess pore water pressures, even after an elapsed

time of 26 seconds. This migration could result in additional movements and potential instability of the abutment as a result of the increase in pore water pressures in the densified zone. Due to this risk, a long term analysis having a duration of 240 seconds was performed for the case of the 39-meter-wide densified zone having 85 percent relative density and extending from 8 meters in front of the embankment toe to 19 meters behind the crest (Case J). This particular case was selected because the densified zone width was the smallest of the cases where predicted abutment deformations were near the tolerable range, thereby making it the most susceptible to pore pressure migration effects.

Figure 8.24 presents time histories of the excess pore water pressure ratio at Points P2 and P10 for the 39-m-wide densified zone case. These points are located under the full-height embankment in the untreated and densified zones at depths of about 4.5 meters below the embankment bottom (refer to Figure 8.3 for locations). Likewise, the excess pore pressure ratio predicted at Points P8 and P11, which are located in the free-field and in the densified zone under the embankment toe, are presented in Figure 8.25. It is apparent from Figures 8.24 that no increase in excess pore water pressure occurred at Point P10 in the densified zone after strong shaking stopped at about 13 seconds. However, at Point P11 in the densified zone near the embankment toe there was a small increase in the excess pore pressure after 13 seconds, as shown in Figure 8.25, with the pressure ultimately peaking at about 70 seconds. The fact that the excess pore pressure ratio peaked at P11 after shaking stopped can probably be attributed to the point being near the untreated free-field which completely liquefied, resulting in a large potential for migration in that area. On the other hand, in the untreated zone under the embankment excess pore water pressure ratios greater than 0.5 only developed below 5 meters depth (relative to the top of the liquefiable soils), with lower pore pressure ratios existing near the surface. Therefore, there was less potential for the excess pore water pressure migration into the densified zone in this area, including at Point P10.

Plots of the number of elements with fully mobilized strength versus time for the untreated and densified zones in the liquefiable strata, as well as the embankment, are presented in Figure 8.26. As seen from this figure the number of elements with fully mobilized strength in these zones initially increased and then decreased with time. Even though the number of these elements initially increased with time, the pattern of the elements was never sufficient to cause additional horizontal and vertical movement of the abutment beyond the 7 and 4.5 centimeters

predicted at the end of 26 seconds. Therefore, excess pore water pressure migration was not sufficient to change the predicted performance of the abutment in this case.

Despite the fact there were no increases in the movements of the stub abutment between times of 26 and 240 seconds, at 180 seconds the pattern of elements with fully mobilized strength in the embankment, between the abutment and toe, was approaching a continuous failure plane. This pattern is illustrated in Figure 8.27. Some of the increase in elements with fully mobilized strength in this area may have been due to stress redistribution in the grid, which is likely more of a numerical than physical phenomena. However, some of the increase could have been due to the softening of the densified zone at the boundary with the liquefied soils in the free-field due to excess pore water pressure migration. This behavior, including the development of a nearly continuous failure plane, suggests that installing vertical drains near this boundary might be warranted to reduce the potential of post-earthquake abutment failure.

8.4.3 Implications for Use

The results of the parametric study analyses indicate that a densified zone can be used to limit the horizontal and vertical movements of a stub abutment supported on an approach embankment over liquefiable soils to tolerable levels for conditions similar to those in the test problem. A densified zone having a high relative density of 85 percent and on the order of 40 to 50 meters wide was necessary to reduce the abutment movements to the acceptable range. As shown in the next section on chemical grouting, treatment of the full-depth of liquefiable soils is necessary to limit movements to tolerable levels.

The analyses performed indicate that acceptable performance of the stub abutment was only obtained when the densified zone was placed under the slope of the embankment and extended out beyond the toe and behind the crest of the embankment. When the treated zone under the slope was only extended beyond the toe or only behind the crest, unacceptable movements were predicted, regardless of the lateral extent of the treatment. The results also seem to indicate that a larger portion of the densified zone should be located under the full-height section of the embankment than outside the toe to be more effective in reducing abutment movements. This observation can probably be attributed to the higher confining stresses in the portion of the densified zone under the embankment allowing greater strength and stiffness to be developed than in the portion outside the embankment.

Excess pore water pressure migration, particularly in the vicinity of the embankment toe, appears to be a potential concern for stability of the densified zone and supported embankment. No post-earthquake failure or increase in movements of the stub abutment for the test problem bridge was predicted after the end of strong shaking due to excess pore water pressure migration. However, it appeared that a pattern of failed elements approaching a continuous failure surface developed between the stub abutment and toe of the embankment after strong shaking stopped. Protection against additional post-shaking movement or failure of the abutment due to pore pressure migration could likely be provided using vertical drains.

Despite the predicted success of using a densified zone to mitigate the effects of liquefaction on the test problem stub abutment, the size of the required zone was large. The size of the improved zone needed for acceptable performance of the stub abutment could potentially be reduced using a method such as chemical grouting.

8.5 Chemical Grouting

8.5.1 Properties and Factors

The performance of improved zones created under the stub abutment and approach embankment using chemical grout consisting of sodium silicate was investigated. The primary factor varied in the analyses for the chemically-grouted zone was the width and location of treatment. All of the analyses assumed the zone extended from the base of the embankment to the bottom of the liquefiable soils at 11-m depth, with the exception of one case where a partial treatment depth in the liquefiable soils was evaluated.

The chemically-grouted material for the stub abutment case was modeled in the same manner and with the same property values used for the bridge pier cases. A summary of the properties used for the grid elements representing the chemically-grouted material is presented in Table 7.5. Some aspects of modeling the material included:

- Using the Mohr-Coulomb failure criteria and hyperbolic stress-strain model to define the strength and deformation behavior;

- Reducing the cohesion to zero in an element upon initial failure in that element leaving only a frictional component of strength;
- Assigning a shear modulus number, K_{2max}, of two times the value for the ungrouted loose sand to the grouted sand, and upon failure in a grouted element, reducing K_{2max} back to the ungrouted sand value; and
- Fixing pore water pressures in the grouted zone elements at static levels so no increase in pore pressure occurs in the zone due to cyclic loading or pore pressure migration.

Additional details regarding the modeling of the chemically-grouted sand in the FLAC analyses can be found in Chapter 7, Section 7.5.1.

The finite difference grid used for analyzing the stub abutment with a chemically-grouted zone in the liquefiable soils was the same as that shown in Figure 8.2. However, two rows of elements representing a dense, non-liquefiable sand layer having a low permeability (relative to the overlying liquefiable sands) and total thickness of two meters were added below those representing the liquefiable soils to allow the grouted block to rock and slide at its base. Properties assigned to this dense sand layer in the FLAC analyses are given in Table 8.3. The dense sand layer was assigned volumetric strain constants, C_1 and C_2, of zero and pore water pressures at the nodes in the layer were fixed at static levels to prevent any unusual or unexpected pore pressure changes in the layer. A low permeability of 5×10^{-7} cm/sec was assigned to the first row of elements representing the loose, liquefiable sand above the dense sand layer to significantly reduce the effect of the static pore water pressures in this layer on those in the overlying soils. The dense sand layer was sufficiently stiff that it did not cause significant amplification of the input base motion.

In determining the initial stress state at the existing abutment prior to shaking, it was assumed that the chemical grouting performed by permeation methods would not change the stress state in the ground. For this reason the initial stress state for the FLAC grid prior to shaking was determined using properties for ungrouted soils under the abutment and approach embankment. Once the initial stresses were determined, the strength and stiffness properties of elements in the grouted zone were changed to those assumed for the grouted material and the velocity record for the scaled Kobe earthquake motion then applied.

8.5.2 Effects on Response and Performance

8.5.2.1 General Effects

The results of the analyses performed indicate that the presence of a chemically-grouted zone in the liquefiable soils beneath an approach embankment supporting a stub abutment can reduce the movements of the abutment significantly compared to the no ground improvement case. This effect was evident in a case where a 26-m-wide chemically-grouted zone was placed beneath the stub abutment and approach embankment of the test problem for the study. In this case one edge of the grouted zone was located 6 meters behind the embankment crest and the other edge 8 meters in front of the embankment toe, as shown in Figure 8.28. The zone extended vertically from the bottom of the embankment to the bottom of the liquefiable soils at 11-m depth (relative to the bottom of the embankment).

Time histories of the vertical (y) and horizontal (x) displacements of Point D1 on the abutment for the 26-m-wide chemically-grouted zone case are presented in Figures 8.29 and 8.30, respectively. The permanent displacements (relative to the base of the grid) predicted at this location at 26 seconds, which is 13 seconds after the end of strong shaking, were 4.2 cm horizontally towards the free-field (positive x direction) and 0.2 cm downward (negative y direction). Approximately 2.9 cm of horizontal displacement was observed between the base of the grid and top of the dense sand layer underlying the liquefiable soils in the vicinity of the grouted zone. This movement indicates some periodic shear failure occurred in the dense sand under the grouted zone during shaking and contributed to the overall horizontal movement of the abutment.

The relatively small horizontal displacement of the abutment relative to the base of the grid in this case indicates that it essentially moved together with the base during shaking. This behavior is further confirmed by the x-velocity time histories of the abutment and base presented in Figure 8.31. As seen from this figure the trends in the two time histories are similar, with very little lag time between the peaks in the base and abutment records. There appears to be some amplification of the simulated earthquake motion as it passes upward from the base, through the improved soils and embankment, to the abutment. The peaks in the velocity record of the abutment are up to 50 percent greater than the corresponding peaks in the input record at the grid base.

Despite the fact that the predicted abutment displacements were relatively small for this case, the excess pore water pressures in the unimproved soils under the embankment were still relatively high, with the excess pore water pressure ratio near the bottom of the liquefiable soils approaching 1.0. The pattern of excess pore water pressures predicted in these unimproved soils was similar to that observed for the 39-m-wide densified zone case presented in Figure 8.15, but the magnitudes were slightly higher.

Like the densified zone case, the chemically-grouted zone appeared to help restrict the development of large shear deformations in the liquefiable soils under the abutment and embankment due to its stiffness and strength. The magnitude of the predicted abutment movements was found to be dependent on the location, size, and depth of penetration of the chemically-grouted zone.

8.5.2.2 Treatment Location and Width

The effect of the chemically-grouted zone location and width on the predicted movements of the stub abutment was investigated through a series of analyses. The analyses were split into four groups in an attempt to systematically determine the more effective treated zone locations and sizes. A summary of the analyses belonging to particular groups is presented in Table 8.4, with each analysis identified as a separate case and assigned a letter designation. The location and lateral limits of the chemically-grouted zone for each case is given in Figure 8.32.

As seen from Figure 8.32, the Group 1 analyses started with a chemically-grouted zone located under the slope of the approach embankment supporting the stub abutment (Case A). This initial location was selected based on the findings of Riemer et al. (1996) from numerical analyses on the effectiveness of different locations and sizes for ground improvement, as discussed in greater detail in Chapter 3, Section 3.2.1.1. The remaining analyses in the group focused on the effect of increasing the treated zone size by moving the treated zone boundary at the embankment toe outwards and away from the embankment. A plot of the predicted abutment displacements versus the distance of the treated zone boundary from the embankment toe is presented in Figure 8.33. The plot shows there was not a substantial improvement in performance by moving the boundary to a location 17 meters from the toe (Case C) or even to the end of the grid (Case D), as compared to having it 11 meters away from the toe (Case B).

In the Group 2 analyses the boundary of the chemically-grouted zone outside the embankment was fixed at 11 meters from the embankment toe based on the Group 1 results. The boundary at the embankment crest was moved to other positions behind the crest along the full-height section of the embankment, as shown in Figure 8.32, producing larger treated zone widths. The data in Figure 8.34 show that increasing the treated zone width by moving the boundary farther behind the crest resulted in a decrease in the predicted movements of the stub abutment to values below the tolerable limit of 5 cm. Based on the results in Figure 8.34 moving the treated zone boundary under the embankment a distance of 6 meters behind the embankment crest, giving a total treatment width of 29-meters (Case E), gave acceptable abutment displacements.

Group 3 analyses were performed to determine if the size of the grouted zone used for Case E in Group 2 could be reduced by moving the grouted zone boundary outside of the embankment closer to the embankment toe, without significantly changing the predicted performance of the abutment. Locations of the boundary at distances 8 and 5 meters from the toe (Cases G and H) were evaluated, with the boundary under the embankment fixed at 6 meters behind the crest. The results presented in Figure 8.35 indicate that moving the boundary outside the embankment progressively towards the toe caused the predicted abutment movements to become progressively larger. However, it appears that moving the boundary from 11 to 8 meters from the toe (Case G) did not substantially change the predicted abutment movements, with the predicted horizontal and vertical movements of 4.3 cm and 0.2 cm, respectively, still being in the tolerable range.

Finally, three analyses were performed in Group 4 to confirm that a slightly different treatment zone location and size than those used for Case G would not improve the predicted performance of the abutment. The location and sizes of the improved zone for the three cases analyzed are shown in Figure 8.32 and summarized in Table 8.4. The first case analyzed, with a grouted zone having a width of 23 meters (Case I) and slightly different position than in Case G, resulted in horizontal movements of the abutment nearly three times the value obtained for Case G. The second treatment case (Case J) had predicted movements similar to Case G, but the treated zone for the former was approximately 3 meters wider. In the last case the grouted zone had a total width of 24 meters and extended from the toe of the embankment to a distance 12 meters behind the crest. This case also had horizontal abutment displacements more than three

times those obtained for Case G, with the displacement pattern in the vicinity of the abutment similar to the one presented in Figure 8.19 for a densified zone case. Based on these analyses the 26-m-wide chemically-grouted zone in Case G, with the zone boundaries located 8 meters in front of the embankment toe and 6 meters behind the embankment crest, appeared to provide the best balance between the zone size, location, and predicted abutment movements.

The results of the above analyses indicate that the chemically-grouted zone in liquefiable soils under the approach embankment and stub abutment in the test problem had to extend some distance both behind the embankment crest and in front of the toe. Treating all of the liquefiable soils under the slope and outside the embankment, as done in Case D, did not reduce the horizontal displacement of the abutment to well within the tolerable range, as seen from the displacement vectors presented in Figure 8.36. In this case, the stiff grouted soil outside the embankment caused failure of the grouted soil to be focused in the upper part of the treated zone under the embankment slope, with the resulting movements occurring to the right and slightly upward toward the slope face. This pattern of failure and ground movement was likely the result of the embankment exerting pressures on the underlying softened, liquefiable soils (due to excess pore water pressure development), which in turn pushed in the direction of the least resistance (i.e. - towards the embankment slope face). This type of behavior was seen in shaking table tests performed by Yanagihara et al. (1992) involving a clay embankment on liquefiable sand with a densified treatment zone at the embankment toe, as discussed in Chapter 3, Section 3.2.1.1. On the other hand for the 26-m wide treated zone used in Case G, horizontal movements occurred over the full-depth of the treated zone, as shown by the displacement vectors in Figure 8.37. Approximately 2.9 cm of the horizontal movement shown by the vectors in the figure was due to periodic shear failure of the dense sand beneath the improved zone during shaking indicating the tendency of the grouted block to periodically slide. Despite the displacement that occurred at the base of the grouted zone, and the additional deformations and grouted soil failure within the zone, the predicted movements of the supported abutment in Case G were only about 50 percent of those in Case D, and within the tolerable range.

8.5.2.3 Treatment Depth

The effect of the chemically-grouted zone thickness on the abutment performance was investigated. One analysis was performed for a 29-m wide zone having the same location as Case E, but extending only to a depth of 8.6 meters below the top of the liquefiable soils

supporting the embankment. The predicted horizontal displacement of the stub abutment for this case was over 1 meter, with most of the deformation concentrated in the untreated zone between the bottom of the grouted zone and the bottom of the liquefiable soils. On the other hand, the predicted horizontal displacement was 2.9 cm when the grouted zone was extended to the bottom of the liquefiable soils (Case E). Based on this analysis, it appears a treated zone that does not fully penetrate the liquefiable soil layer beneath a stub abutment and approach embankment will result in excessive movements of the abutment. This undesirable behavior is largely due to the inability of the untreated, liquefiable soils beneath the treated zone to resist the shear forces induced in the ground by the abutment and embankment. The inadequacy of a partially-penetrating improved zone for liquefaction remediation in sloping ground was also observed in numerical analyses by Yasuda et al. (1991), as mentioned in Chapter 3, Section 3.2.1.2.

8.5.2.4 Extended Duration

The results presented above for the grouted zone cases were for analyses having a time duration of 26 seconds, which is approximately 13 seconds beyond the end of the strong shaking. To confirm that a longer term failure of the abutment would not occur, analyses having durations up to 205 seconds were performed for the 26-m-wide chemically grouted zone with boundaries at 6 meters behind the embankment crest and 8 meters in front of the toe, respectively (Case G). In the results of this analysis, there was no noticeable increase in the movement at point D1 on the abutment between 26 seconds and 205 seconds. There was a minor increase in settlement at the back of the abutment of less than 0.5 millimeters per minute, but the rate appeared to be decreasing at the end of 205 seconds. This settlement did not appear to be significant.

Figure 8.38 presents the number of elements with fully mobilized strength in different parts of the grid with time. The figure indicates an increase in the number of these elements in the grid up to a time of 120 seconds, despite the fact that pore water pressures inside the grouted zone were fixed at static levels and pressures in the untreated zones were decreasing after 26 seconds. The reason for this increase in the number of failed elements is not readily apparent, but may be associated with some stress re-distribution in the finite difference grid after strong shaking stopped at about 13 seconds. After 120 seconds, there is a significant decrease in the number of elements with fully mobilized strength in the untreated liquefiable soils and only minor increases in the grouted zone and the embankment. Based on these trends, it appears the

system has stabilized by about 120 seconds and a longer term failure for this particular case is unlikely.

8.5.3 Implications for Use

The results of the analyses performed for chemically-grouted zones indicate that this ground improvement method could likely be used for liquefaction-mitigation at a stub abutment and approach embankment having conditions similar to the test problem. The width of the grouted zone required to reduce the abutment movements to tolerable levels in the test problem was at least 13 meters less than the required width for a densified zone at 85 percent relative density, indicating smaller treated zone sizes are likely possible with chemical grouting than densification. Like the densified zone, the chemically-grouted zone could not be located only under the embankment slope, but had to extend both behind the embankment crest and in front of the toe to reduce abutment movements to tolerable levels. For the test problem a chemically-grouted zone having a total width of 26 meters and extending behind the crest and in front of the toe distances of 6 and 8 meters, respectively, resulted in tolerable movements. Treating only under the slope and in front of the toe, or only under the slope and behind the crest, resulted in unacceptable movements.

Some of the horizontal movement of the abutment and embankment that occurred was due to some periodic shear failure of the dense sand underlying the grouted zone. This shear failure appears indicative of the tendency for periodic slip to occur between the grouted block and underlying soil during shaking.

One analysis performed of a grouted zone extending only partially into the liquefiable soil layers indicates a partial treatment depth will result in unacceptable movements. The grouted zone must fully penetrate the liquefiable soils. This observation regarding treatment depth likely applies to other ground improvement methods as well, such as densification by compaction grouting or cementation by jet grouting.

In analyzing the performance of the stub abutment and approach embankment supported with a chemically-grouted zone, a number of simplifying assumptions were made. A particularly important assumption was that no excess pore water pressure develops in the grouted zone during dynamic loading, although there is laboratory test data showing that saturated, chemically-grouted soil can liquefy due to cyclic loading (Maher et al., 1994). In addition, no increase in pore water pressure was allowed in the grouted zone due to migration from untreated

zones, even in portions of the zone where the grout failed. As mentioned in the last chapter, future improvements in the modeling of chemically-grouted soil for liquefaction remediation should include a pore pressure generation model for the grouted soil and accounting for the changes in its groundwater flow properties. These improvements will help provide an even better evaluation of chemical grouting for liquefaction remediation at stub abutments.

8.6 Jet Grouting

8.6.1 Properties and Factors

The use of jet grouting at the stub abutment and approach embankment was investigated to see if the size of the treated zone in the liquefiable soils producing tolerable abutment movements could be reduced in comparison to the densified and chemically-grouted zones. Figure 2.8 provides an illustration of the general configuration used for the jet-grouted zone at the stub abutment. The replacement ratio for the zone was assumed to be 100 percent such that a solid block of jet-grouted material was present.

The properties and modeling approach used for the jet grouted material in the stub abutment case were the same as the pier case. Some key aspects of modeling the material included:

- Using a Mohr-Coulomb failure criteria and a linear elastic-perfectly plastic stress-strain model to define the strength and deformation behavior;
- Assuming an unconfined compressive strength of 15000 kPa for the jet-grouted material and taking the cohesion and tensile strength as 15 and 10 percent of the compressive strength, respectively;
- Taking Young's modulus as approximately 300 times the unconfined compressive strength and computing the shear and bulk moduli assuming a Poisson's ratio of 0.3;
- Reducing the cohesion to zero upon initial failure; and
- Assuming no pore pressure changes in a jet-grouted element, before or after failure of the element, due to cyclic loading and pore water pressure migration from untreated zones.

More details regarding the modeling and properties of the jet-grouted material are provided in Chapter 7, Section 7.6.1.

The finite difference grid used for modeling the stub abutment and approach embankment with a jet-grouted zone in the liquefiable soils underneath them was the same as shown in Figure 8.2. However, like the analyses for the chemical grouting cases, two additional rows of elements were added to the bottom of the grid representing a dense, non-liquefiable sand layer having a low permeability (relative to the overlying liquefiable sands) and a total thickness of two meters. The properties and behavior assumed for the dense sand were the same as those used in the chemical grouting analyses, as described in Section 8.3.2.

Installation of a jet-grouted zone at a stub abutment for liquefaction remediation likely causes changes in the stress state around the abutment and approach embankment. For this reason, in the FLAC analyses the stress state existing in the ground prior to earthquake shaking was approximated by including the jet-grouted zone in the liquefiable soils prior to applying the embankment and abutment loads. After the stress state due to placement of the embankment and abutment were determined, the simulated earthquake record was then applied to the base and sides of the grid.

In the parametric study analyses conducted for the jet-grouted zone, the only variable investigated was the distance the zone extended laterally underneath the embankment from the embankment toe. The grouted zone was assumed to extend downward through the liquefiable soils under the embankment and penetrate a distance of one meter into the underlying dense sand layer.

8.6.2 Effects on Performance and Response

The effects of jet-grouted zones having widths of 5.5, 12, and 15 meters on the predicted stub abutment movements were investigated. The location of these treated zones and the predicted movements for the abutment in each case are presented in Figure 8.39. In all of the cases, some horizontal displacement of the abutment towards the free-field is predicted, as well as some vertical displacement. The magnitude of the movements become smaller as the distance the grouted zone extends under the embankment from the toe increases. No failure occurred in the elements representing the jet-grouted material in all three cases. Based on an upper limit for tolerable predicted movements of about 5 cm, the predicted movements for the grouted zone

widths of 5.5, 12, and 15 meters would likely be considered unacceptable, marginal, and acceptable, respectively.

The mechanism causing the ground deformations and abutment movements associated with the jet grouting improvement is apparent from the displacement vectors in the vicinity of the stub abutment for the 5.5-meter-wide zone presented in Figure 8.40. This figure illustrates that the jet-grouted wall had a tendency to rotate about one edge of its base like a rigid body subjected to overturning. As the distance the wall extended beneath the embankment increased, the forces resisting the periodic increases in overturning forces during shaking increased, resulting in reduced permanent movements of the wall, and thus the embankment and abutment.

Figures 8.41 and 8.42 present time histories of the horizontal and vertical movements predicted at Point D1 (refer to Figure 8.28 for location) on the abutment for the 15-m-wide jet-grouted zone. The plot in Figure 8.41 indicates that the oscillations of the abutment in the horizontal direction became progressively more biased in the positive x-direction after about 7 seconds of elapsed time. The magnitude of the oscillations got larger at about 8 seconds, with the relative displacement ranging from 0 to 5 cm, before reaching a final horizontal displacement of 2.6 cm at the end of strong shaking. On the other hand the vertical movement of the abutment progressively increased starting at a time of about 4 seconds, with most of the 1.2 cm of upward displacement occurring after 7 seconds. The upward movement was a result of the jet-grouted block, which extended underneath the abutment, rotating upwards.

As shown in Figure 8.43, the predicted horizontal (x) velocity record at point V1 (refer to Figure 8.28 for the location) on the abutment for the 15-m-wide grouted zone case had similar trends to the input velocity record, with the abutment velocity only lagging a small fraction of a second behind the input velocity. The peaks in the velocity record of the abutment were up to 50 percent larger than those in the input record.

Predicted excess pore water pressure ratios in the untreated liquefiable soils under the embankment generally had the same trends as shown in Figure 8.15 for one of the densified zone cases. In general, the magnitudes of the excess pore pressure ratio for the jet-grouted zone case were slightly higher than those shown in Figure 8.15. The excess pore water pressure ratio predicted in the untreated soils increased with depth below the bottom of the embankment, reaching 1.0 near the bottom of the liquefiable soils.

Like the chemically-grouted zone, the jet-grouted zone helped to limit movements of the abutment by containing and limiting the shear deformations that occurred in the liquefiable soils under the embankment that were softened due to the development of excess pore water pressures during shaking. The limitation of the deformations is dependent on the strength and stiffness of the jet-grouted zone, which in the cases evaluated did not fail, and its ability to resist the increased overturning forces during shaking.

No analyses of the jet-grouted zones were performed for durations longer than 26 seconds. The potential for longer term movements of the stub abutment and approach embankment due to continued ground distortion and failure of the grouted zone seemed unlikely because none of the jet grouted material failed and the pore water pressures in the untreated foundation soils started decreasing immediately after shaking stopped. For the 5.5-m and 12-m-wide jet-grouted zone cases, there is the potential for densification of the untreated soils behind the zone having some effect on the stub abutment since these zones do not extend behind the back of the abutment. However, this was not evaluated because the abutment movements for these two cases were either unacceptable or marginal.

The performance of the jet-grouted zone in the analysis was dependent in part on the assumption there was no increase in pore water pressures in the zone above static levels. Although this assumed behavior seems reasonable given the nature of the jet-grouted material and the fact that it did not fail, some further study of this issue might be warranted.

8.6.3 Implications for Use

The analyses performed for liquefaction remediation at a stub abutment using jet grouting indicate that the abutment movements can be reduced to acceptable levels for cases having conditions similar to those assumed in the test problem. In the test problem the treated zone width needed to reduce abutment movements to tolerable levels was approximately 11 meters smaller for jet grouting than needed for chemical grouting and 24 meters smaller than densification by compaction grouting. Therefore, jet grouting appears more desirable than chemical and compaction grouting from the standpoint of reducing the size of the treated zone while still maintaining tolerable abutment movements. Like chemically-grouted and compaction grouted zones, a jet-grouted zone will likely be only effective in reducing abutment displacements when it fully penetrates the liquefiable soil layers. These results appear consistent with observations by Yasuda et al. (1991) from shaking table tests and numerical analyses

involving the effects of different remediation measures on the movements of sloping ground, as discussed in Chapter 3, Section 3.2.1.2.

The performance of a jet-grouted zone is highly dependent on its strength. In the parametric study the strength assumed for the jet grouted material was high and resulted in no material failure during shaking. Selecting a jet grouting mixture such that failure of the material does not occur during shaking appears desirable to limit the size of the treated zone needed at the stub abutment. If failure of the jet-grouted material does occur, in a fashion similar to that observed for the chemically-grouted cases analyzed, a larger treatment width will be needed to maintain adequate performance of the abutment.

In the parametric study performed the jet-grouted zones were all located under the embankment. For the jet-grouted zone width of 15-meters in the study, the zone could have potentially been shifted slightly toward the free-field so that it was located partly outside the embankment. However, this move would likely have caused larger predicted abutment movements because the forces resisting overturning of the grouted block during shaking are reduced. A jet-grouted zone that will not fail during shaking is probably most effective when located completely under the embankment for this reason. In addition, as a zone of given width is moved further out from under an embankment, the potential increases for the untreated soil under the embankment to push outward towards the slope face, thereby increasing movements. Moving the jet-grouted zone out from under the abutment also increases the potential for densification settlements in the untreated soil behind the wall from having some effect on the abutment.

A narrow jet-grouted wall at the embankment toe that penetrates deep into a non-liquefiable layer beneath the liquefiable soils will not likely be successful in limiting movements. Although the deep embedment of the wall will limit overturning movements, there is an increased potential for failure of the jet grouted material. Even if the deeply embedded wall does not fail due to the overstressing, excessive movement of the abutment is still possible due to the softened, untreated liquefiable soils beneath the embankment pushing laterally and upward toward the embankment slope. In addition, densification of the liquefiable soils under the embankment could negatively affect the abutment.

8.7 Buttress Fill

8.7.1 Properties and Factors

The final ground improvement method investigated for the stub abutment on an approach embankment consisted of a buttress fill placed in front of the embankment slope. The objective of a buttress fill is to increase the liquefaction resistance and stiffness of the liquefiable soils by increasing the effective stresses in the ground. In addition, the buttress fill provides additional mass to resist a potential slope stability failure and increases the length of a potential failure surface.

Only one buttress fill case was analyzed. The fill had a width of 8 meters and a height of 3.6 meters. This size was selected based on the constraints imposed by the clearance under the bridge and the location of the first pier adjacent to the abutment in the test problem.

The buttress fill material was assumed to be the same as the gravelly sand of the approach embankment. The Mohr-Coulomb failure criteria was used to define the strength behavior of the material. The shear stress-strain behavior of the fill was defined using the hyperbolic model by Pyke (1979), as formulated in the Pyke-Byrne model for FLAC. No pore water pressure was allowed to develop in the buttress fill during cyclic loading because of the its location above the groundwater table, which was at the top of the liquefiable soils. Properties used for the buttress fill in the dynamic analyses are the same as those presented in Table 8.1 for the embankment material.

The finite difference grid used in the FLAC analyses of the stub abutment with the buttress fill was the same as that shown in Figure 8.2 with the exception that additional elements were added in front of the embankment to represent the buttress. Figure 8.44 shows the grid in the vicinity of the stub abutment with the buttress fill elements included.

The initial stress state for the buttress fill case was established by first determining the stress induced in the liquefiable soils due to placement of the approach embankment and stub abutment. After that phase of the analysis was complete, the rows of elements representing the buttress fill were sequentially placed from bottom to top resulting in the remediated abutment configuration. The velocity record simulating earthquake shaking was then applied to the base and sides of the grid.

8.7.2 Effects on Performance and Response

Figures 8.45 and 8.46 present the time histories of predicted horizontal and vertical movements for Point D1 on the stub abutment. The predicted permanent displacements of the abutment are 89 cm horizontally toward the free-field (positive x direction) and 36 cm downward (negative y direction). These movements are large and very similar to those obtained for the case of no improvement of the liquefiable soils (refer to Figures 8.5 and 8.6). They are not tolerable for a bridge such as the one in the test problem.

Although the predicted displacements of the stub abutment with the buttress fill were essentially the same as the no improvement case, some changes were seen in the pore water pressures in the liquefiable soils and ground movements along the full-height section of the approach embankment. The predicted excess pore water pressures in the liquefiable soils immediately beneath the buttress were somewhat lower than the no improvement case, particularly at shallow depths. In addition, the vertical and horizontal movements at the top of the embankment were reduced by about 5 cm and 10 cm, respectively, at distances of about 15 meters and more behind the abutment.

8.7.3 Implications for Use

Based on the results of the one analysis performed, it appears using a buttress fill having a width and height of only a few meters probably will not improve the performance of a stub abutment supported on an approach embankment over thick deposits of liquefiable soils. The additional effective stresses induced in the liquefiable soils in the vicinity of the buttress do not appear sufficient to dramatically affect the excess pore water pressure development, and associated softening, in these soils. Therefore, it is unlikely that a buttress fill will significantly reduce the predicted movements of the stub abutment compared to the unimproved case. In essence, the buttress fill only moved the slope face farther from the abutment, but did little to change the behavior of the liquefiable soils under the abutment.

Although a buttress fill may not be effective at a stub abutment and approach embankment on thick deposits of liquefiable soils, such as those in the test problem, it could potentially be effective for the case where the liquefiable layer is relatively thin and at shallow depth. It may particularly be effective if a key trench is excavated through the liquefiable soils and backfilled with compacted material prior to placing the buttress fill. The use of the buttress fill for this case should be investigated in future research work.

8.8 Insights Regarding Remediation at Stub Abutments

Based on the results of the parametric studies performed for the stub abutment supported on an approach embankment underlain by liquefiable soils with and without improved ground zones, insights have been gained regarding the use of compaction grouting, chemical grouting, jet grouting, and buttress fills to improve the abutment performance. These insights, which apply to bridge and site conditions similar to the test problem, are summarized below.

- Improved ground zones must be properly positioned and have adequate size, strength, and stiffness to (1) reduce the large shear deformations that occur in the liquefiable soils under and immediately outside the approach embankment during shaking when no ground improvement is in place, (2) prevent a localized slope stability failure at the abutment and embankment slope leading to substantial downward and outward movements of the abutment and (3) resist the tendency of untreated, weakened liquefiable soils under the embankment from pushing laterally and upwards toward the embankment slope. Providing ground improvement to limit movements due to one or two of the above mechanisms will cause the remaining mechanism(s) to dominate the deformation behavior of the system. Therefore, the improvement scheme must be balanced, limiting deformations associated with all three mechanisms.
- The size and location of the treated ground zone needed to limit deformations associated with the above-mentioned mechanisms to acceptable levels is dependent in part on the strength and stiffness properties of the improved material. The stronger and stiffer the treated material, the smaller the width of treatment that is needed. In general, the treated zone in the liquefiable soils under the approach embankment needs to extend laterally under the stub abutment and the embankment slope. In addition, the zone must extend downward through all of the liquefiable soil layers.
- For remediation using chemical grouting and densification by compaction grouting the treated zone beneath the abutment and embankment slope likely needs to extend a limited distance behind the stub abutment (i.e. - under the full-height of the

embankment) and a limited distance outside the embankment (i.e. - beyond the embankment toe). Increasing the treatment width by expanding the improved zone in either direction helps limit the shear deformation in the liquefiable soils. Extending the treated zone out beyond the toe of the embankment also helps to reduce the potential of a localized slope stability failure at the abutment and embankment slope. Expanding the treated zone behind the stub abutment reduces the potential of the weakened, untreated soils under the embankment pushing laterally and upward towards the embankment slope.

- For both densified and chemically-grouted improved zones there appear to be limits to the effectiveness of expanding the treated zone boundaries on the abutment performance. As the treated zone boundaries are moved farther behind the embankment crest or farther in front of the toe, the predicted movement of the abutment progressively decreases but the incremental reduction in the predicted displacement, with the increasing treated zone width, gets progressively smaller. A point is eventually reached where the additional reduction in the predicted abutment movements is not sufficient to justify the increase in the treated zone size and cost.
- Densification improvement using compaction grouting can be used to limit horizontal movements of the stub abutment to 5 to 10 cm and, likewise, the vertical movements to 5 to 10 cm. However, it appears the liquefiable soils must be improved to a relatively high relative density (i.e. – on the order of 85 percent) and the width of treatment must be relatively large (i.e. - on the order of 40 to 50 meters for the test problem evaluated).
- Chemical grouting can potentially reduce the size of the treated zone needed at an abutment in comparison to densification. In addition, the lower limits of vertical and horizontal abutment movements that can be achieved using chemical grouting appear to be smaller than those for densification by compaction grouting.
- Jet grouting producing high strength material can further reduce the size of the treated zone needed under an abutment in comparison to chemical grouting. Although the jet-grouted material may not fail during shaking, displacements can still be large due to periodic increases in the overturning forces during the seismic event resulting in incremental movements of the grouted block and abutment. Therefore the jet-grouted

zone likely needs to extend under most of the embankment slope and perhaps even behind the stub abutment to limit this incremental movement caused by overturning forces.

- A narrow jet-grouted wall installed at the toe of an approach embankment and penetrating deep into non-liquefiable strata beneath liquefiable soils will not likely be successful in limiting abutment movements to tolerable levels due to potential overstressing and failure of the wall, ground movement toward the embankment slope, and densification of the untreated soils beneath the abutment.
- A limited size buttress fill placed at the toe of an approach embankment supported on thick, liquefiable deposits does not appear effective in reducing abutment movements. This type of remediation might be effective if the liquefiable layer is thin and at shallow depth and the buttress fill is used in conjunction with a compacted fill key trench, but more research is needed for this treatment scheme.
- In the parametric study, excess pore water pressure migration into the densified zones having acceptable movements at the end of strong shaking did not result in additional movements or failure of the stub abutment after strong shaking stopped. However, over time there was an increase in the number of elements with fully mobilized strength between the abutment and toe of the embankment suggesting such a failure might be possible. For densified zones that only extend a few meters beyond the embankment toe the potential for this failure should be evaluated. Installing vertical drains somewhere between the embankment toe and edge of the densified zone could reduce the likelihood of this failure.
- The development of pore water pressures in the chemically grouted zone due to cyclic loading or pore pressure migration from untreated zones was not incorporated in the analyses performed due to the limited information available to model these phenomena. Future research work should incorporate these phenomena in the analyses for chemically-grouted zones to improve predictions of behavior and check predictions from analyses where the phenomena were not included.
- For some ground improvement methods, such as densification and chemical grouting, there will be overlap of the treated zone for the stub abutment and the adjacent bridge pier. This overlap will necessitate using one combined zone of ground treatment to

support both the abutment and pier. The joint performance of the stub abutment and pier supported together on the combined zone needs to be evaluated in future research.

- The insights gained from the parametric study are applicable to two-dimensional (2-D) cases. As discussed in Section 8.2.6, similar trends in the predicted permanent displacements of the abutment are likely to be seen in three-dimensional (3-D) cases, although the magnitude of the predicted movements might be somewhat different. The applicability of the 2-D results to 3-D cases will be highly dependent on the ground improvement configuration used along the sides of the approach embankment behind the stub abutment. Further research into 3-D effects on the performance of the stub abutment should be pursued.

Overall, the results of the parametric study analyses indicate that compaction, chemical, or jet grouting can be used to limit movements of a stub abutment supported on an approach embankment over liquefiable soils to tolerable levels for conditions similar to the test problem. The insights gained from this study, as well as the study for ground improvement at piers, provide useful information regarding the use and behavior of improved ground for liquefaction remediation at existing highway bridges. This information is summarized again in Chapter 9, along with the lessons learned regarding the factors and phenomena affecting improved ground behavior and the potential of using simplified methods for predicting performance.

TABLE 8.1: Properties Assigned to Approach Embankment Soil [1]

Property	Assigned Value
Relative Density, Dr (%)	81
Unit Weight, γ (kN/m^3): Moist	20.4
Porosity, n	0.23
Hydraulic Conductivity, k (cm/sec)	5×10^{-2}
Friction Angle: Peak, ϕ_p'	38
Dilation, ψ [2]	0.8
Shear Modulus Number, K_{2max}	64
Volumetric Strain Constants[3]: C_1	0.0
C_2	0.0

Notes:
1. Embankment constructed of compacted, clean, well-graded, gravelly sand.
2. Dilation angle only included for zones of embankment located directly over areas of foundation soils which have induced shear stress acting in horizontal direction, τ_{xy}.
3. Embankment located above ground water table, therefore volumetric strain constants of zero were used for it since no pore water pressure would be generated within it and volumetric changes in the embankment material were expected to be small.

TABLE 8.2: Summary of Cases Evaluated for Densified Zone at Stub Abutment

Group	Case [1]	Relative Density, Dr (%)	Total Densified Zone Width [2] (m)	Distance to Boundaries [3] (m)		Abutment Displacement [4] (cm)	
				Behind Crest	In Front of Toe	Horizontal	Vertical
1	A	75	12	0	0	56.0	-15.4
	B	75	68	0	56	30.9	-9.4
	C	75	89	77	0	16.8	-14.7
	D	75	145	77	56	6.8	-6.5
2	E	75	17	0	5	47.9	-9.6
	F	75	20	0	8	38.9	-7.9
	G	75	23	0	11	36.8	-7.4
3	H	75	39.4	19.4	8	14.8	-7.0
	I	75	59	39	8	7.0	-8.0
4	J	85	39.4	19.4	8	7.0	-4.5
	K	85	48.5	28.5	8	6.0 [5]	-7.1 [5]

Notes:
1. Refer to Figure 8.16 for schematic showing location of each case.
2. All densified zone widths include the 12-meter-wide section under the slope of the embankment which extends from the embankment crest (assumed to be at the back of the stub abutment) to the embankment toe.
3. Distance to boundaries of densified zone are given relative to the embankment crest (assumed to be at the back of the stub abutment) and embankment toe.
4. Predicted displacements are for Point D1 on stub abutment.
5. Predicted horizontal and vertical displacements of 4 and -5 cm, respectively, were obtained when accumulated volumetric strains (used in pore pressure generation code) for elements were initialized back to zero before applying dynamic load.

TABLE 8.3: Properties Assigned to Dense Sand Layer at Base [1]

Property	Assigned Value
Relative Density, Dr (%)	75
Unit Weight, γ (kN/m^3): Moist	20.3
Porosity, n	0.36
Hydraulic Conductivity, k [2] (cm/sec)	5×10^{-7}
Friction Angle: Peak, ϕ_p'	37.5
Dilation, ψ	0.0
Shear Modulus Number, K_{2max}	59
Volumetric Strain Constants [3]: C_1	0.0
C_2	0.0

Notes:
1. Dense sand layer having thickness of 2 meters placed below liquefiable soils.
2. Pore water pressures fixed to static values in dense sand layer. First row of elements above the layer assigned a hydraulic conductivity of 5×10^{-7} cm/sec to reduce effect of layer on pore water pressures in overlying liquefiable soils. The layer was assumed to have a low permeability relative to the overlying liquefiable soils.
3. Dense sand layer assumed not to generate any pore water pressure due to cyclic loading induced by shaking.

TABLE 8.4: Summary of Cases Evaluated for Chemically-Grouted Zone at Stub Abutment

Group	Case [1]	Total Grouted Zone Width [2] (m)	Distance to Boundaries [3] (m)		Abutment Displacement [4] (cm)	
			Behind Crest	In Front of Toe	Horizontal	Vertical
1	A	12	0	0	32.8	-5.4
	B	23	0	11	10.2	-1.2
	C	29	0	17	8.6	0.3
	D	68	0	56	10.0	0.5
2	E	29	6	11	2.9	0.4
	F	35	12	11	-1.1	-0.1
3	G	26	6	8	4.3	-0.2
	H	23	6	5	10.5	-1.1
4	I	23	3	8	13.2	-0.1
	J	28.4	3	13.4	4.1	-0.1
	K	24	12	0	15.0	-13.4

Notes:
1. Refer to Figure 8.32 for schematic showing location of each case.
2. All chemically-grouted zone widths include the 12-meter-wide section under the slope of the embankment which extends from the embankment crest (assumed to be at the back of the stub abutment) to the embankment toe.
3. Distance to boundaries of grouted zone are given relative to the embankment crest and embankment toe.
4. Displacements presented for Point D1 on stub abutment.

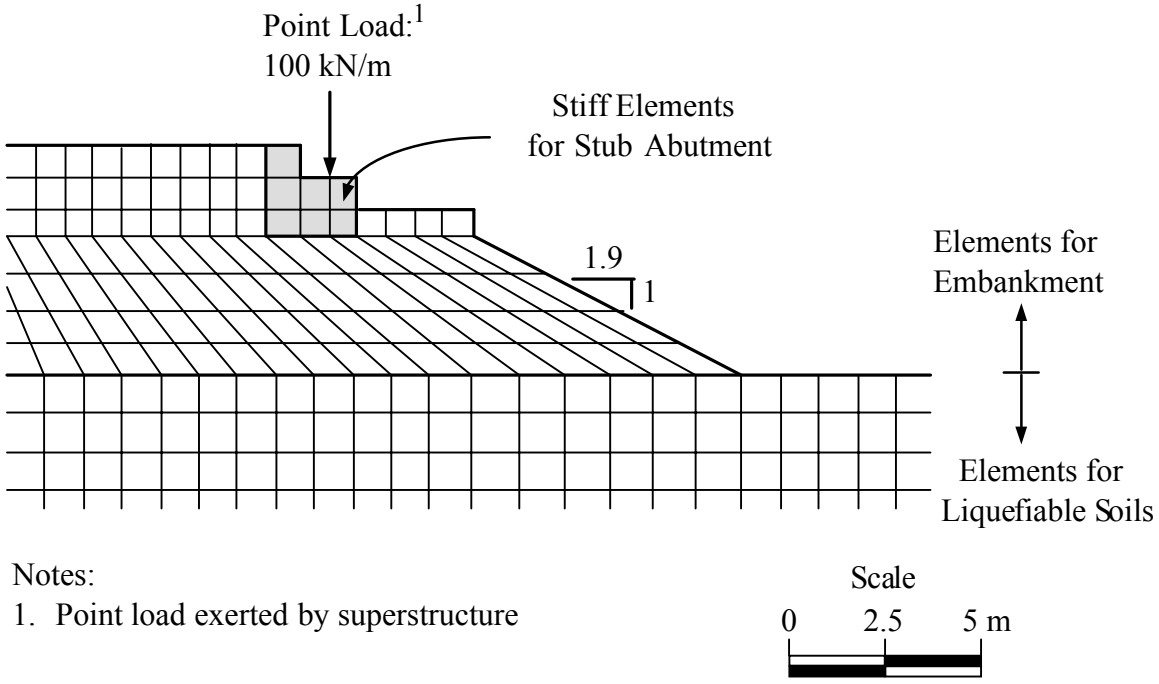

FIGURE 8.1: Representation of Stub Abutment and Superstructure Load in FLAC Analyses

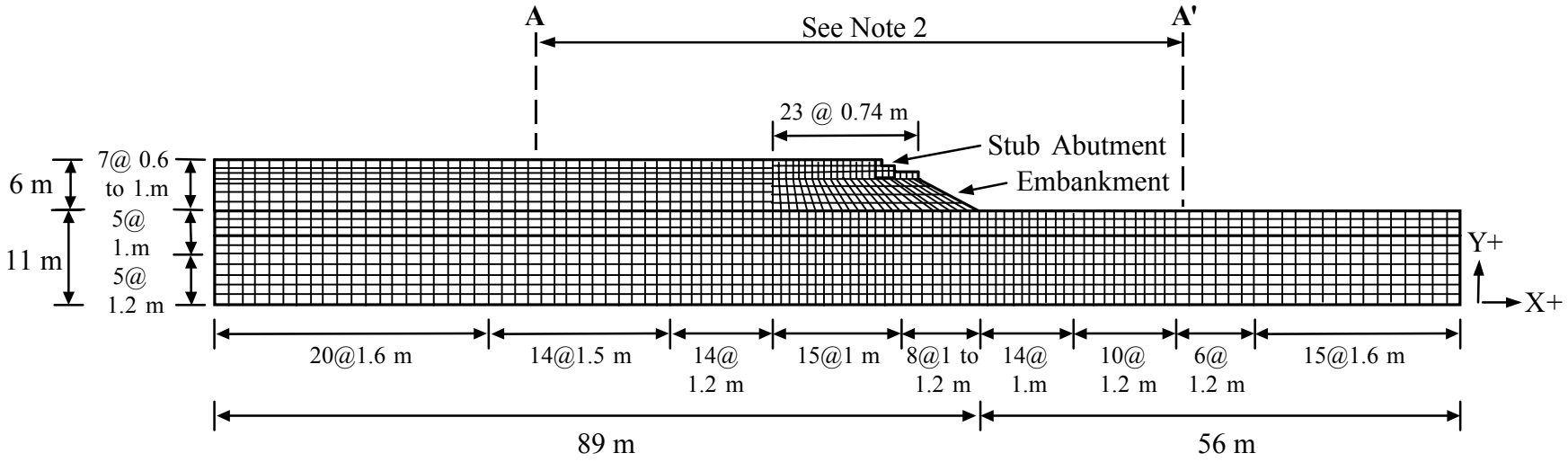

Notes: 1. Horizontal (X) velocity record applied to nodes along bottom and sides of grid.
Bottom of grid fixed in vertical (Y) direction.
2. Section of grid from A to A' presented at larger scale in Figure 8.3.

FIGURE 8.2: Grid Used for FLAC Analysis of Stub Abutment in Parametric Study

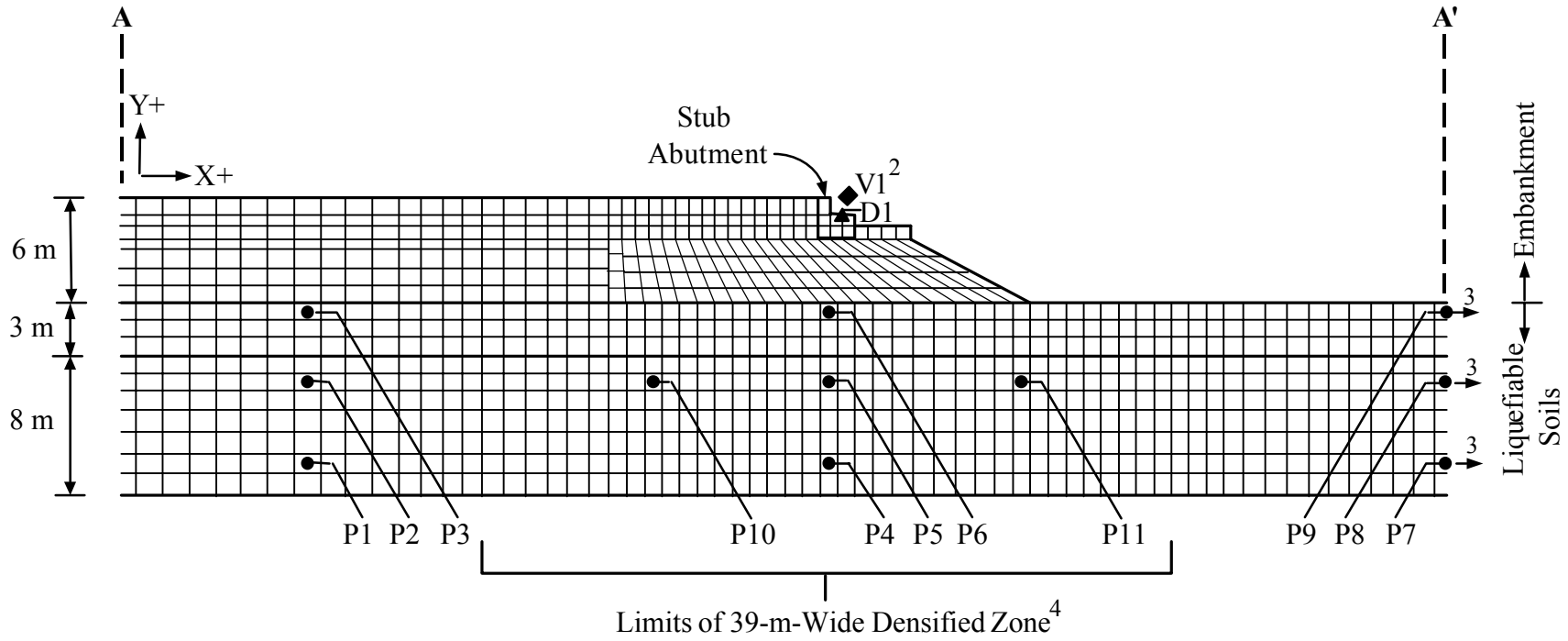

Notes: 1. Symbol indicates a predicted time history for a particular element or node is presented in a figure.
2. V1 shown offset from its actual location, which is the same place as D1.
3. Pore pressure obtained in elements located 15.5 meters from place where symbols shown.
4. Detailed results and discussion presented in text for 11-m-thick densified zone having limits shown, as well as case of no improvement.

FIGURE 8.3: Expanded Section A-A' of Grid Used for FLAC Analysis of Stub Abutment

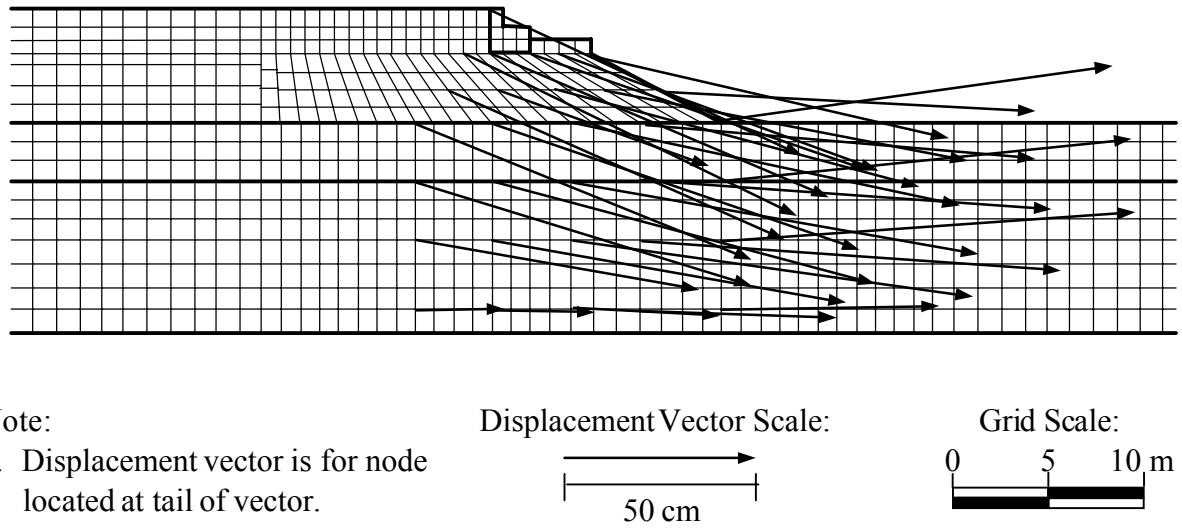

FIGURE 8.4: Displacement Pattern in Vicinity of Stub Abutment for Case of No Ground Improvement

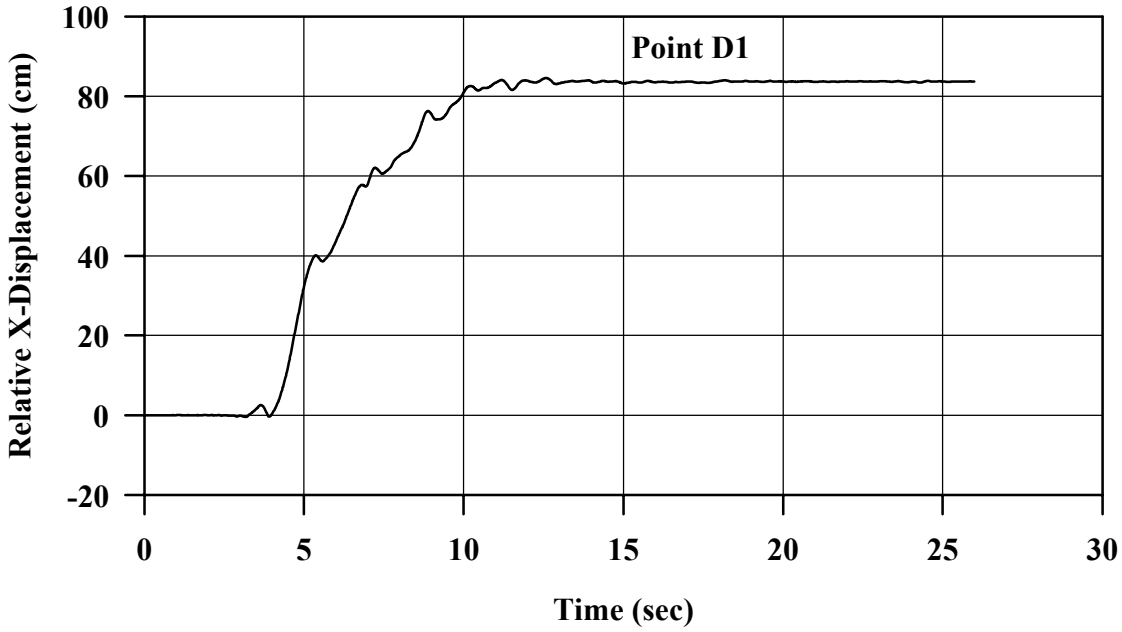

FIGURE 8.5: Relative X-Displacement Between Stub Abutment and Base of Grid vs. Time for No Improvement Case

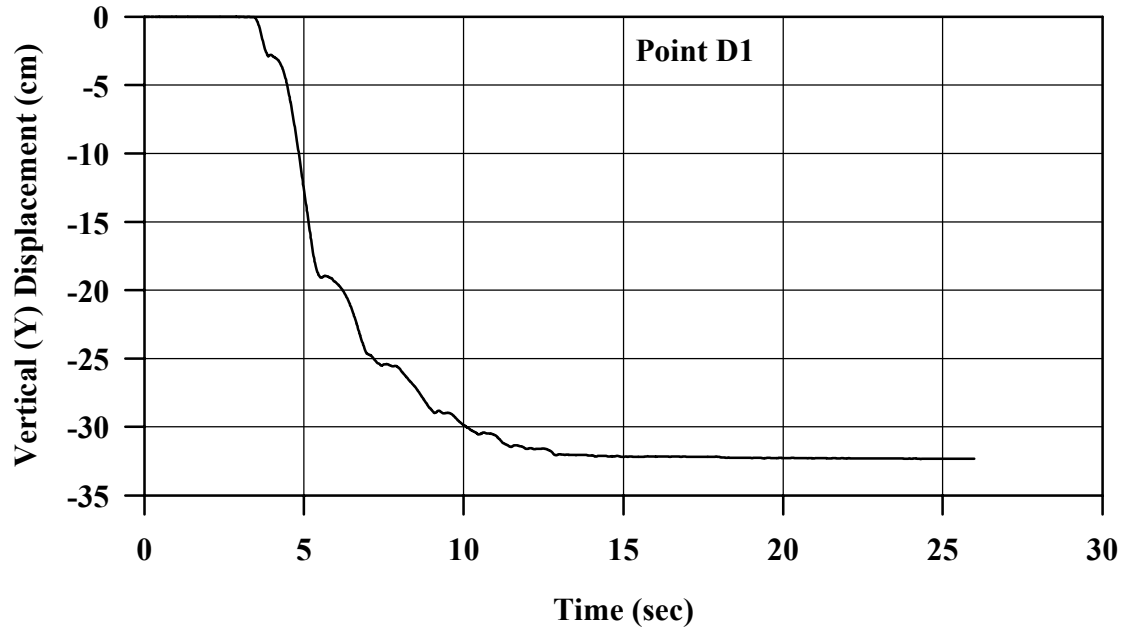

FIGURE 8.6: Vertical Displacement of Stub Abutment vs. Time for No Improvement Case

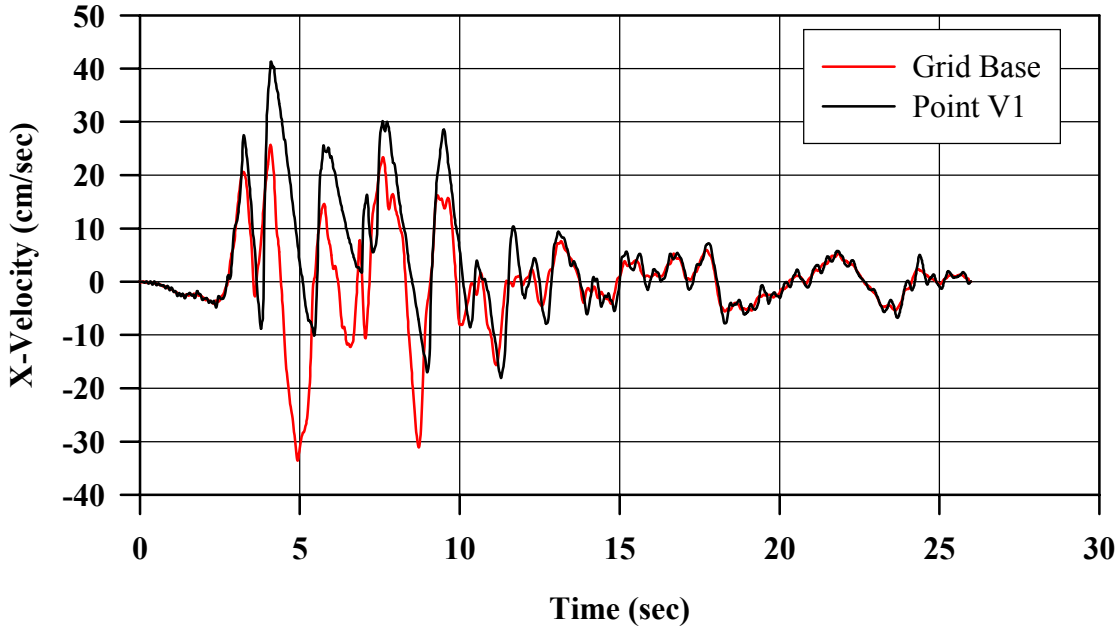

FIGURE 8.7: X-Velocity of Grid Base and Stub Abutment vs. Time for No Improvement Case

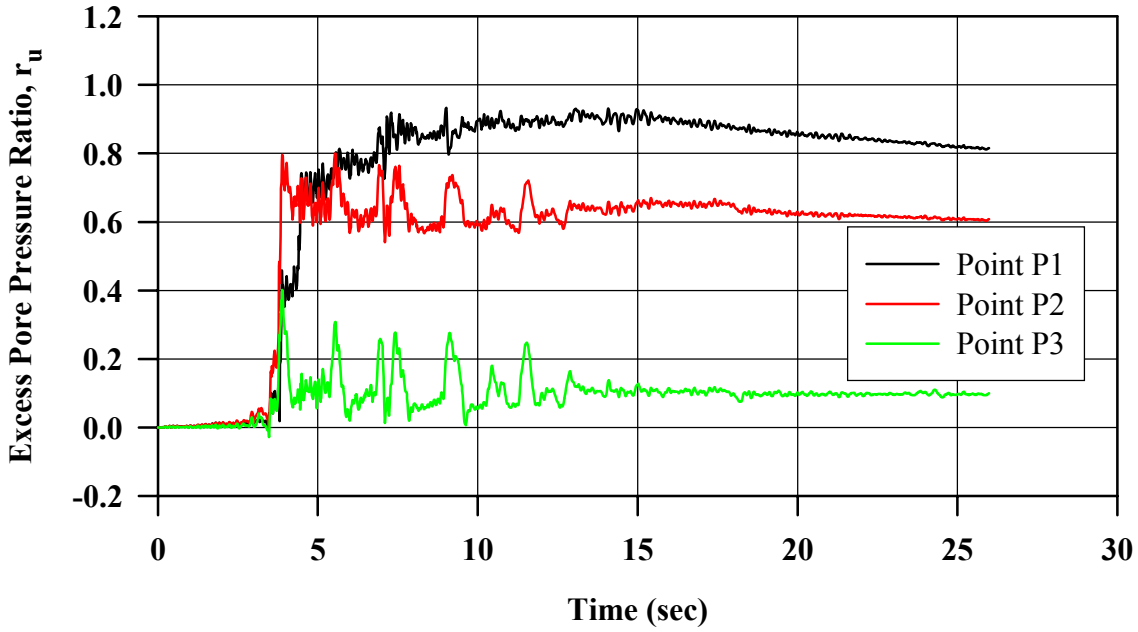

FIGURE 8.8: Excess Pore Water Pressure Ratio Under Embankment vs. Time for No Improvement Case

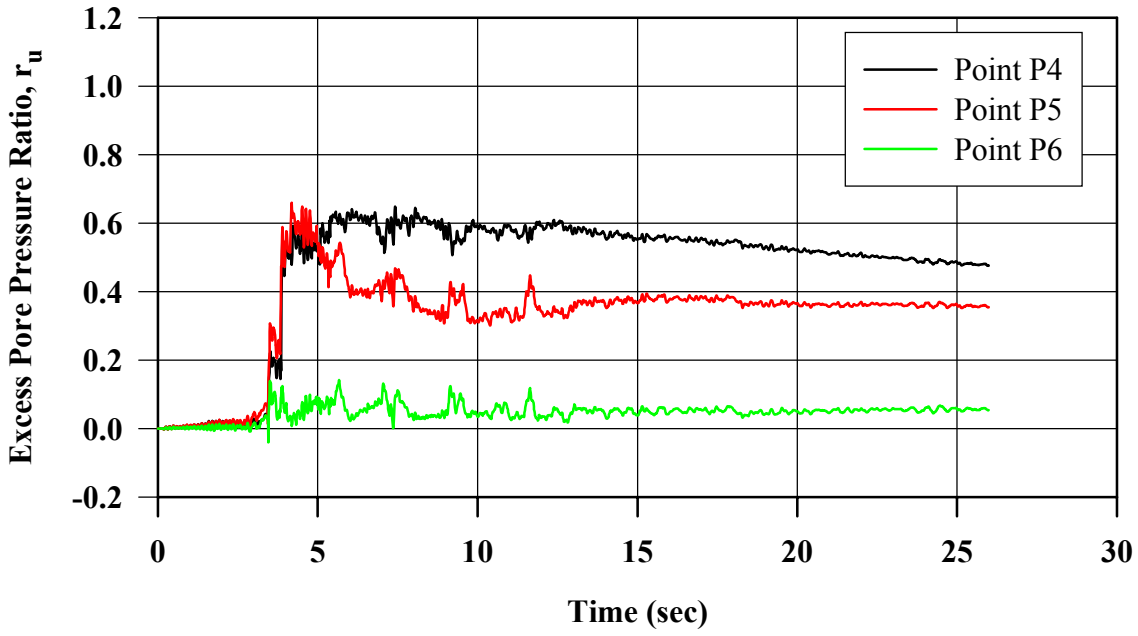

FIGURE 8.9: Excess Pore Water Pressure Ratio Under Stub Abutment vs. Time for No Improvement Case

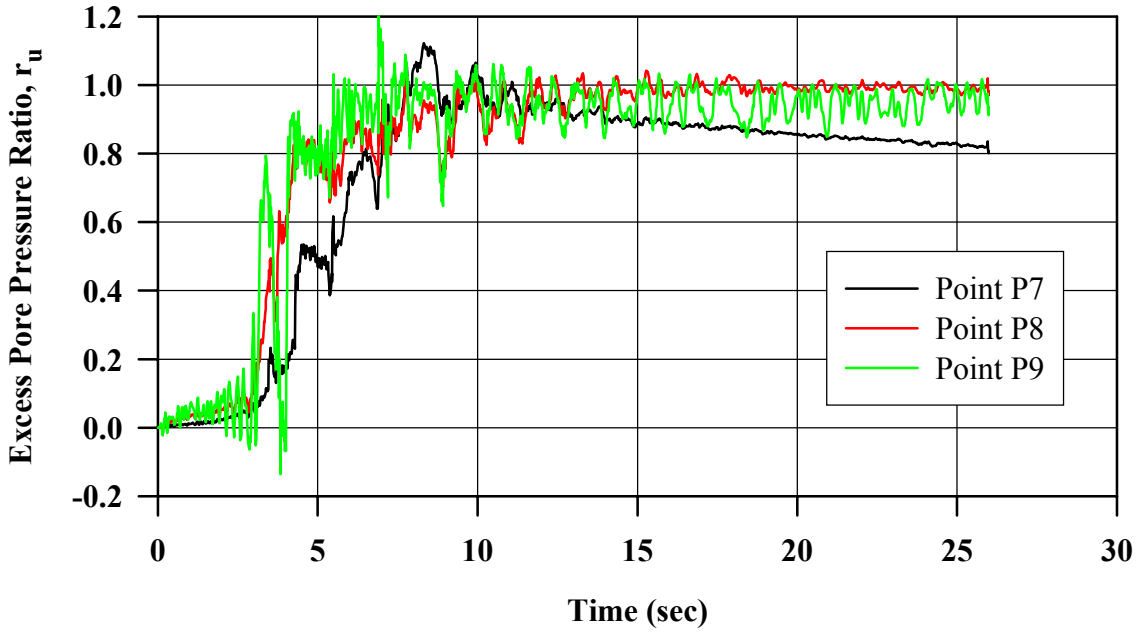

FIGURE 8.10: Excess Pore Pressure Water Ratio in Free-Field vs Time for No Improvement Case

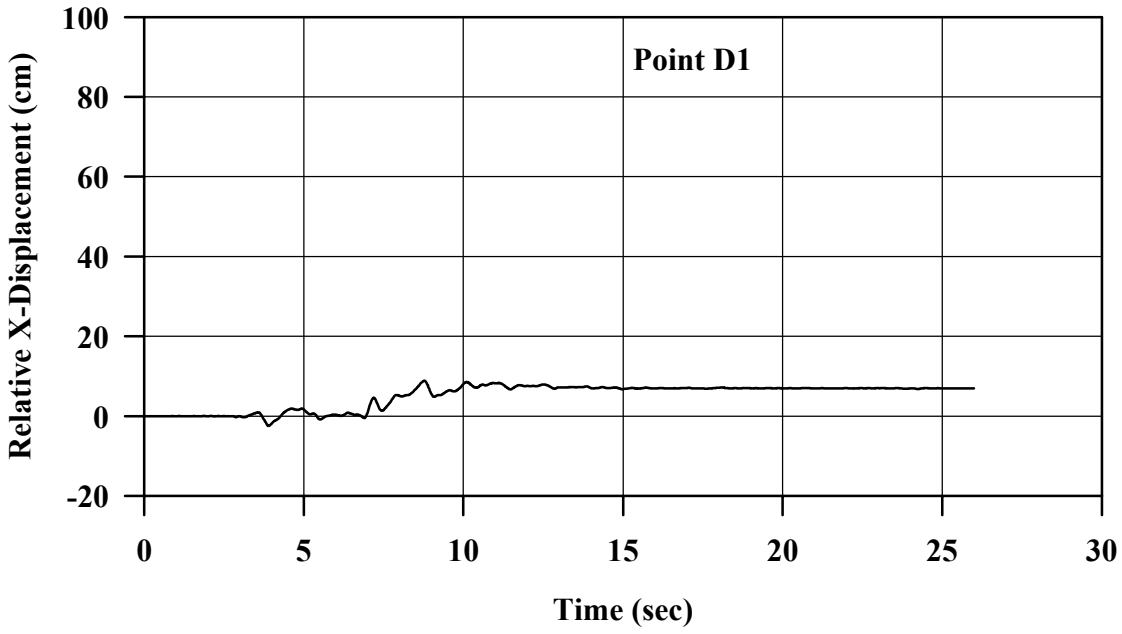

FIGURE 8.11: Relative X-Displacement Between Stub Abutment and Base of Grid for 39-m-wide Densified Zone (Dr = 85%)

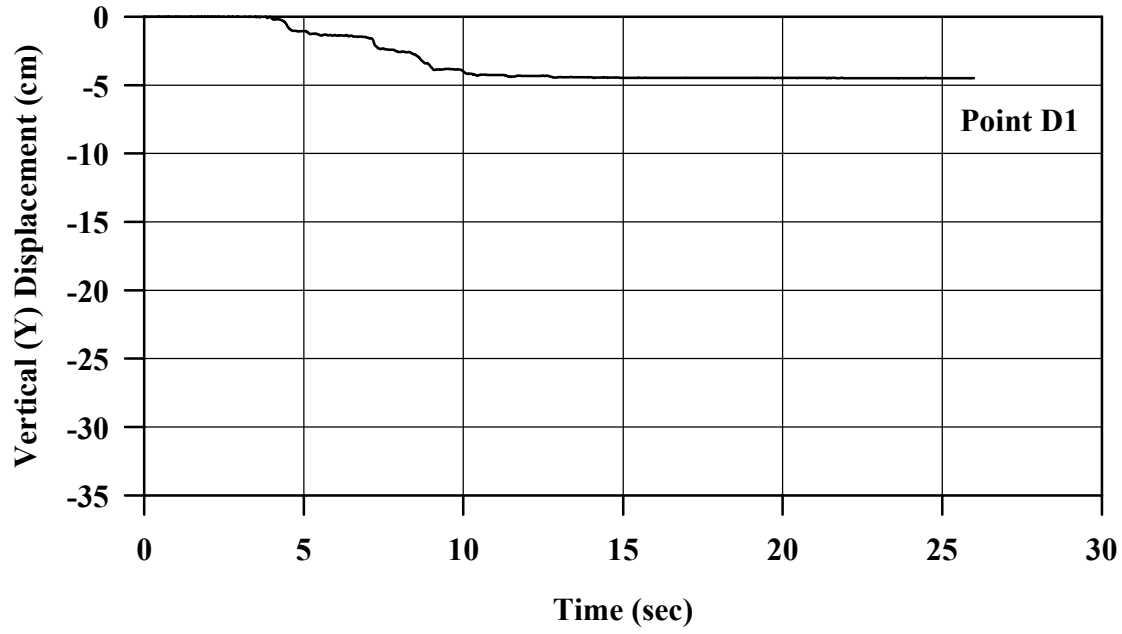

FIGURE 8.12: Vertical Displacement of Stub Abutment vs. Time for 39-m-wide Densified Zone (Dr = 85%)

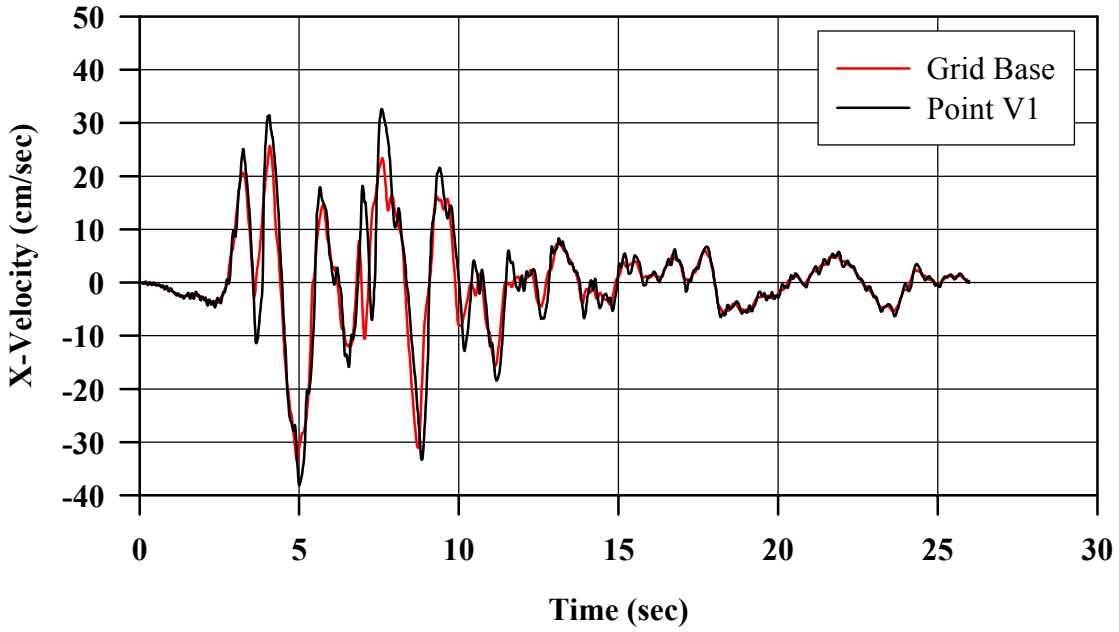

FIGURE 8.13: X-Velocity of Grid Base and Stub Abutment vs. Time for 39-m-wide Densified Zone (Dr = 85%)

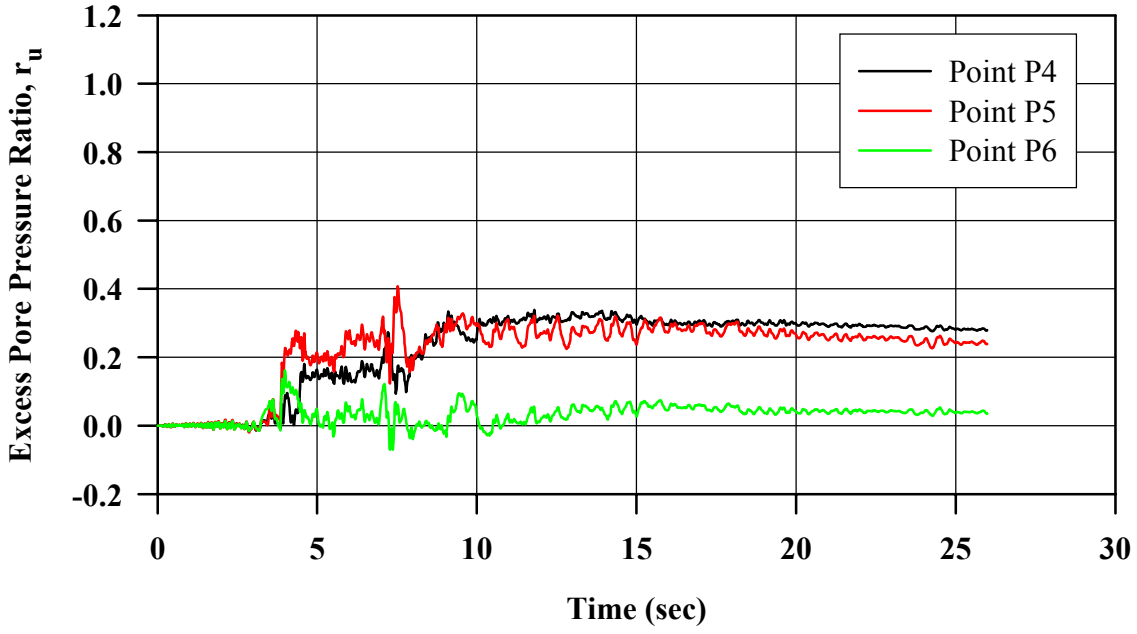

FIGURE 8.14: Excess Pore Water Pressure Ratio in 39-m-wide Densified Zone (Dr = 85%) Under Stub Abutment vs. Time

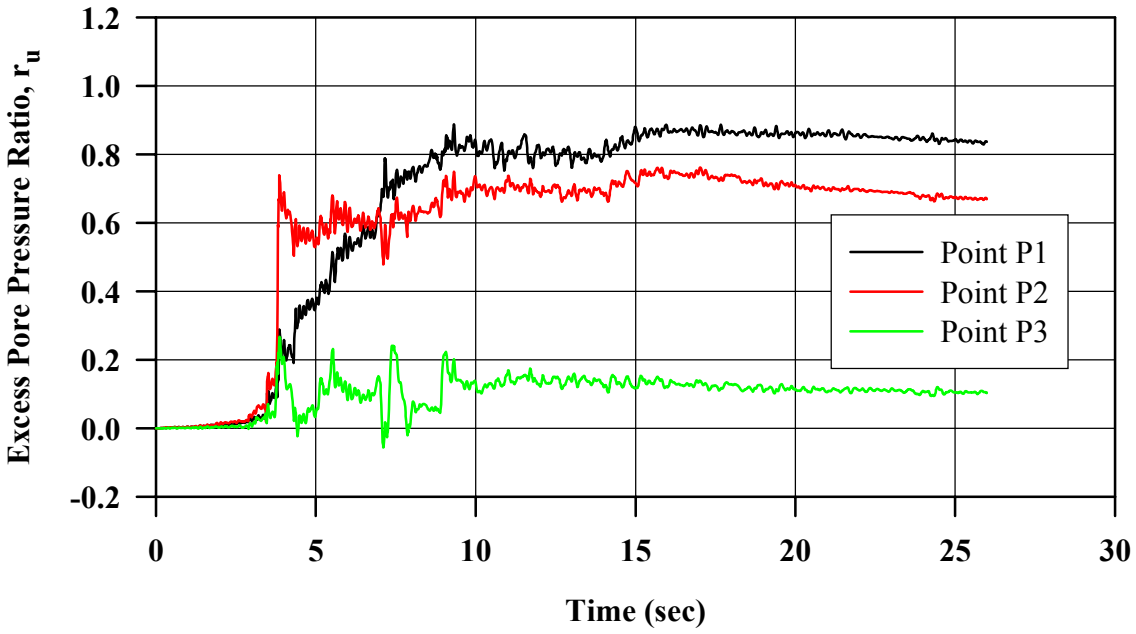

FIGURE 8.15: Excess Pore Pressure Water Ratio in Unimproved Soils Under Embankment vs . Time for 39-m-wide Densified Zone (Dr = 85%)

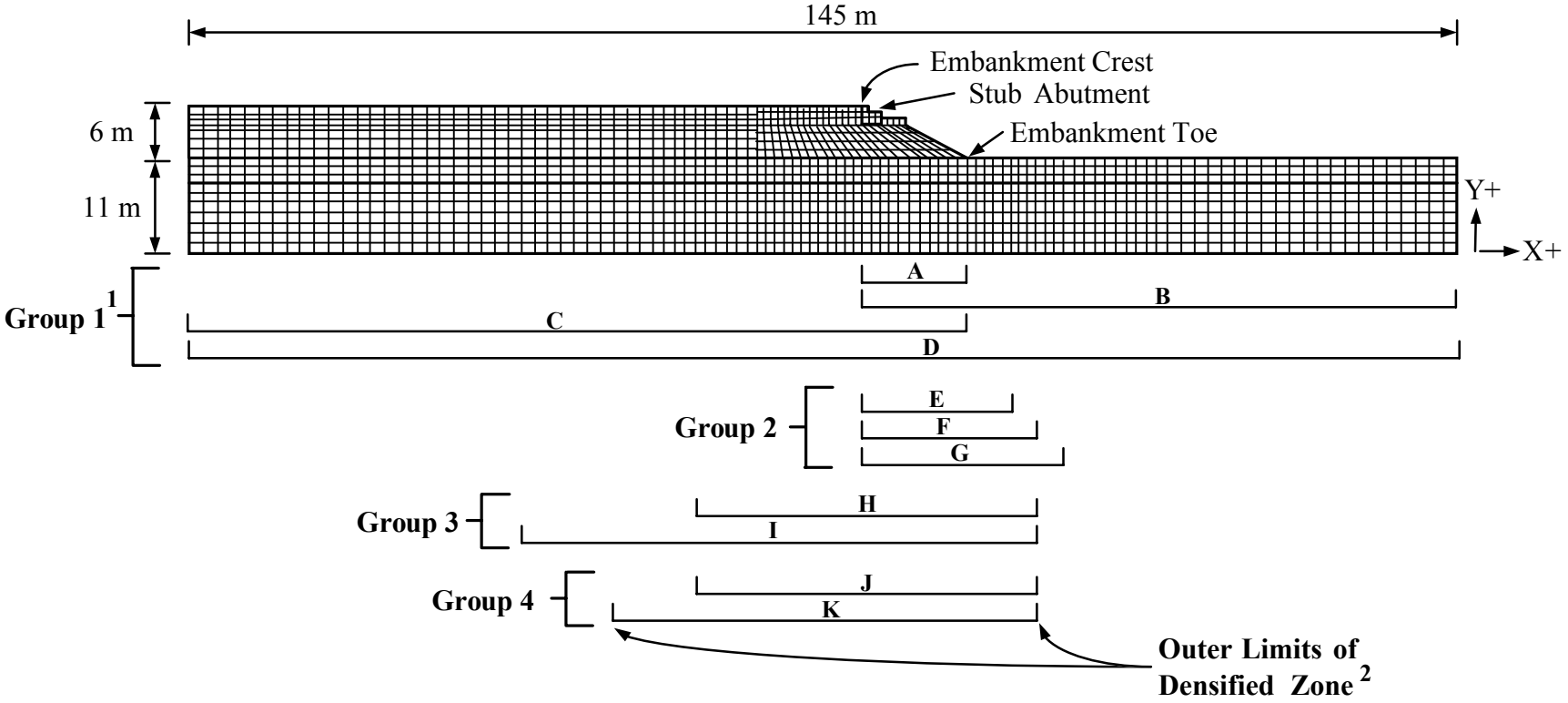

Notes: 1. Groups include analyses performed of abutment with densified zones having different sizes and locations shown (each one is assigned a letter which is used as a reference). Details concerning zone dimensions and locations are provided in Table 8.2. All zones are 11-m-thick, extending from bottom of embankment to bottom of liquefiable soil. Zones consist of sand densified to a relative density of 75 percent, except those in Group 4 which are densified to 85 percent.

2. All sands within outer limits shown are densified.

FIGURE 8.16: Cases Evaluated in Parametric Study of Densified Zones at Stub Abutment

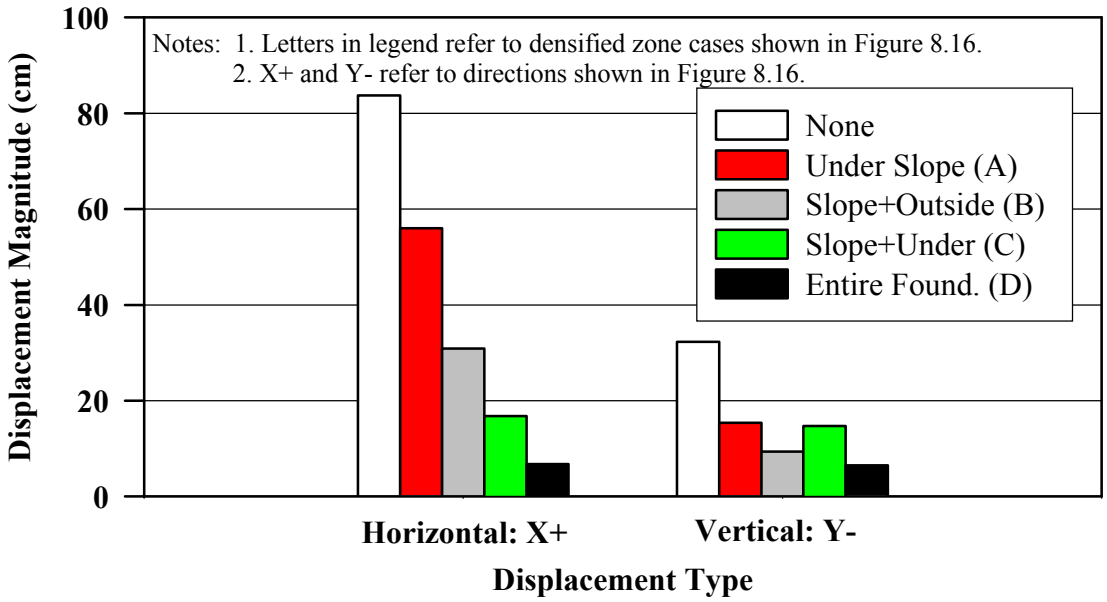

FIGURE 8.17: Variation of Stub Abutment Displacements with Densified Zone (Dr = 75%) Size and Location for Group 1 Cases

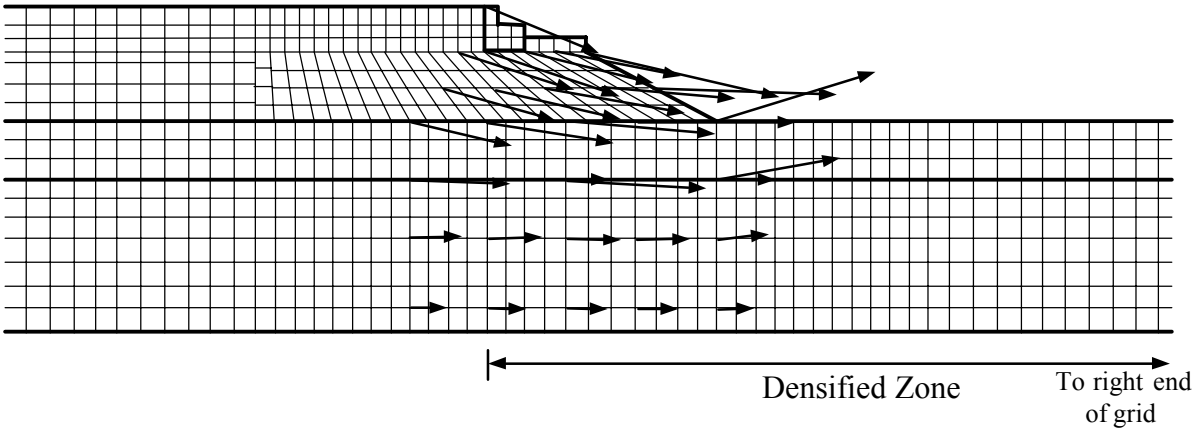

FIGURE 8.18: Displacement Pattern in Vicinity of Stub Abutment for Densified Zone (Dr = 75%) Under Embankment Slope and Outside Embankment (Case B)

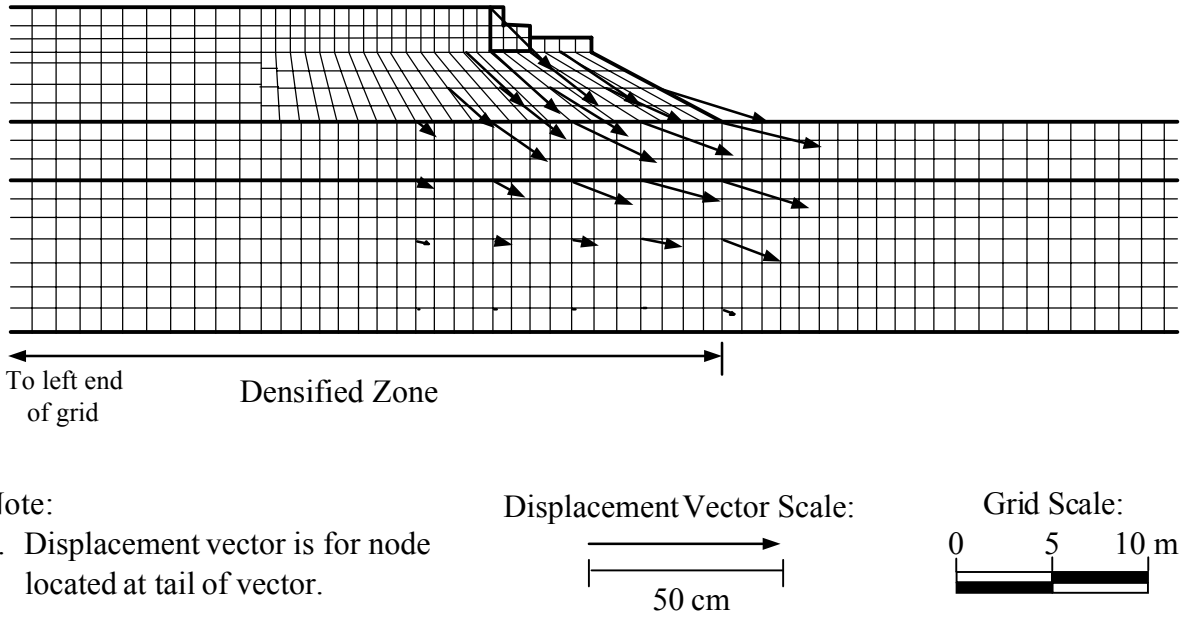

FIGURE 8.19: Displacement Pattern in Vicinity of Stub Abutment for Densified Zone (Dr = 75%) Under Entire Embankment (Case C)

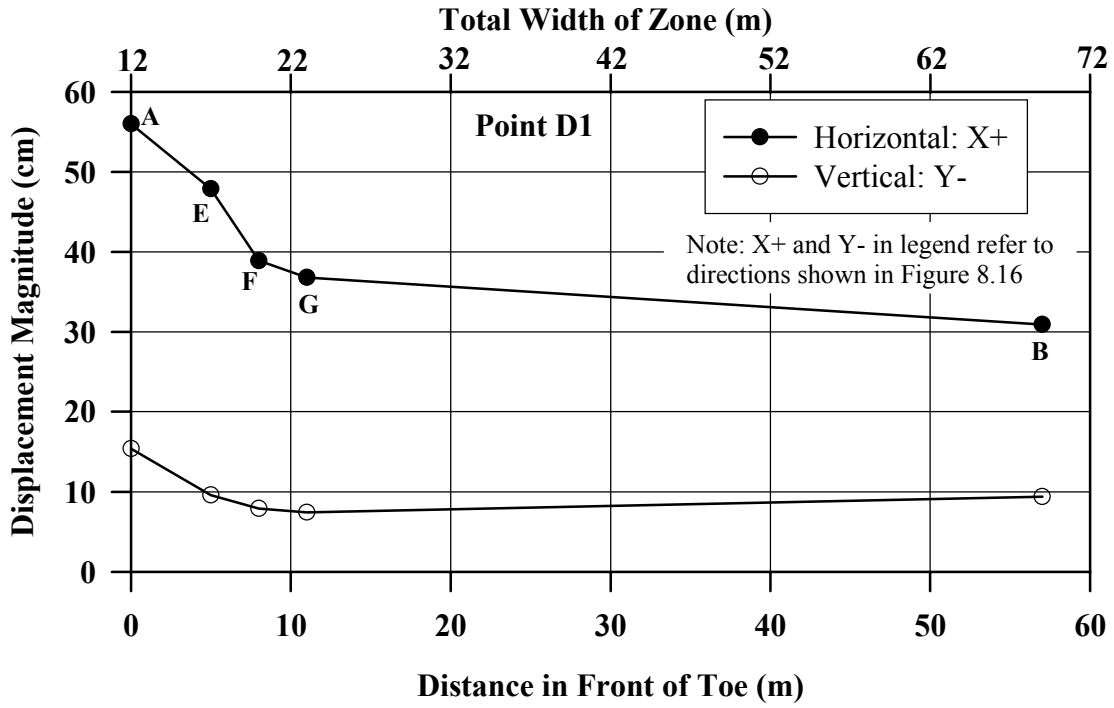

FIGURE 8.20: Displacement of Stub Abutment vs. Distance Densified Zone (Dr =75%) Extends in Front of Toe for Group 2 Cases

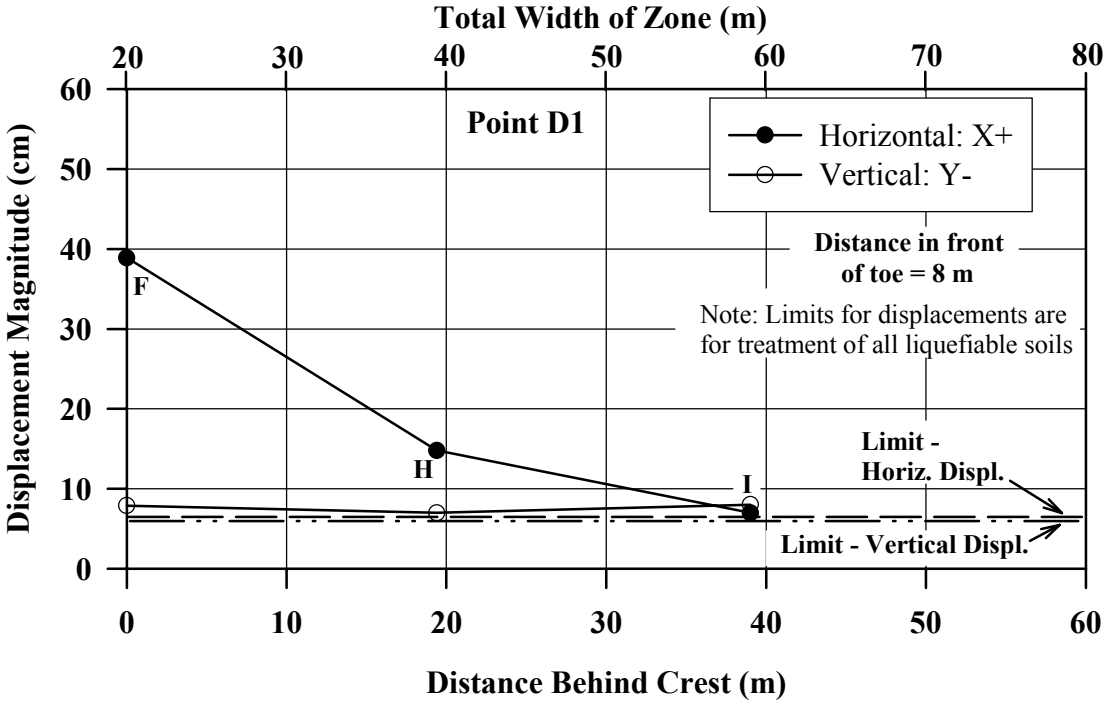

FIGURE 8.21: Displacement of Stub Abutment vs. Distance Densified Zone (Dr = 75%) Extends Behind Crest for Group 3 Cases

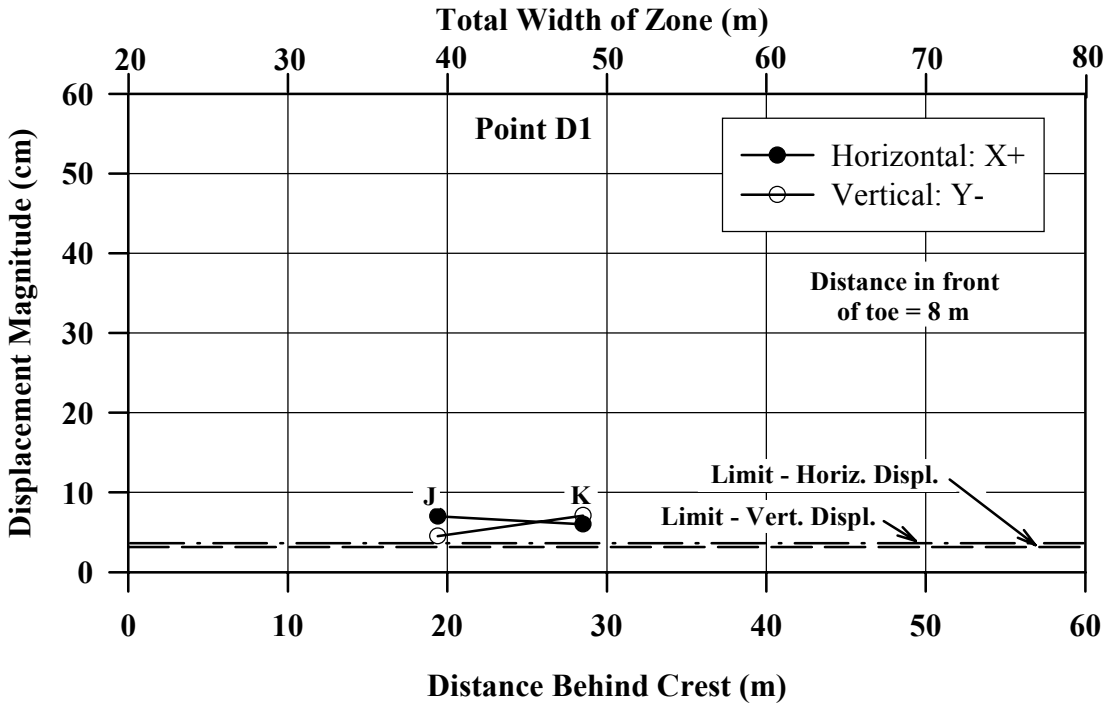

FIGURE 8.22: Displacement of Stub Abutment vs. Distance Densified Zone (Dr = 85%) Extends Behind Crest for Group 4 Cases

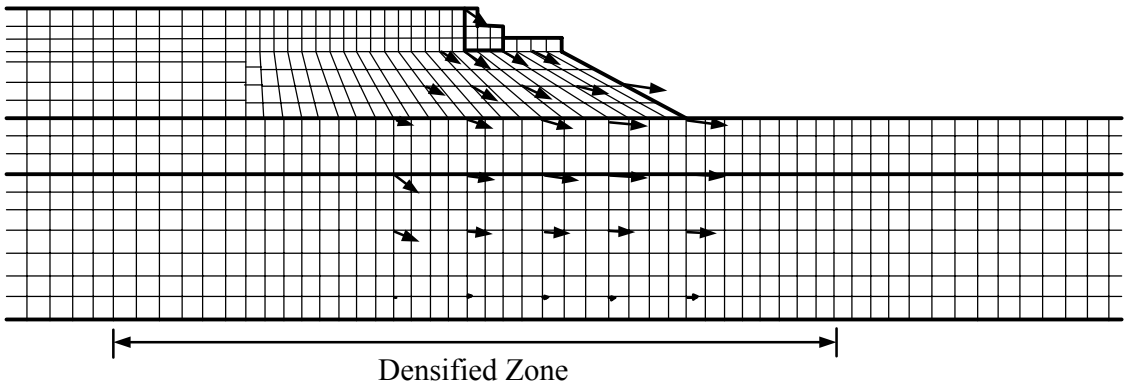

Note:
1. Displacement vector is for node located at tail of vector.

Displacement Vector Scale:

50 cm

Grid Scale:

0 5 10 m

FIGURE 8.23: Displacement Pattern in Vicinity of Stub Abutment for 39-m-wide Densified Zone (Dr = 85%) Starting 19 m Behind Embankment Crest (Case J)

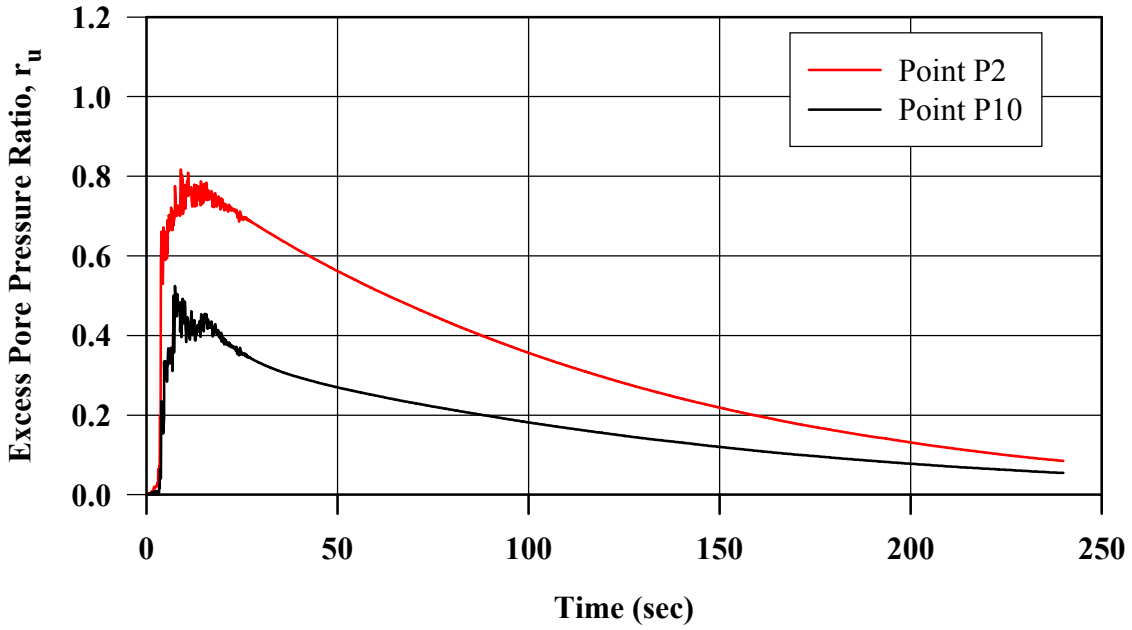

FIGURE 8.24: Excess Pore Water Pressure Ratio Under Embankment in Untreated and Treated Areas for 39-m-wide Densified Zone at Dr = 85% (Case J)

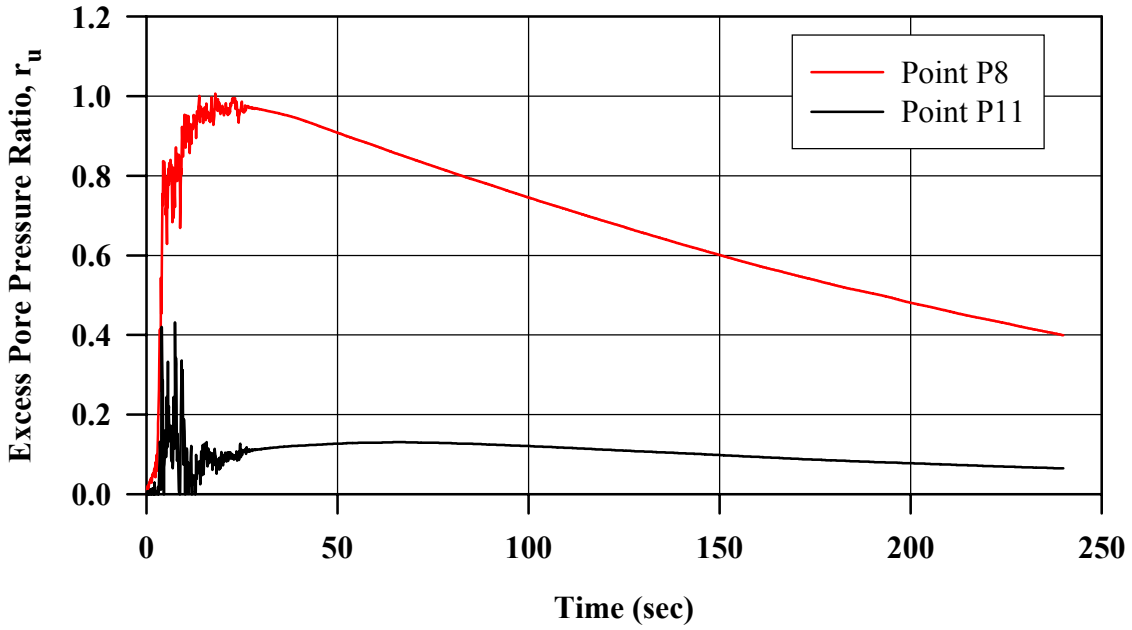

FIGURE 8.25: Excess Pore Water Pressure Ratio in Treated Area at Toe of Embankment and Free-Field for 39-m-wide Densified Zone at Dr = 85% (Case J)

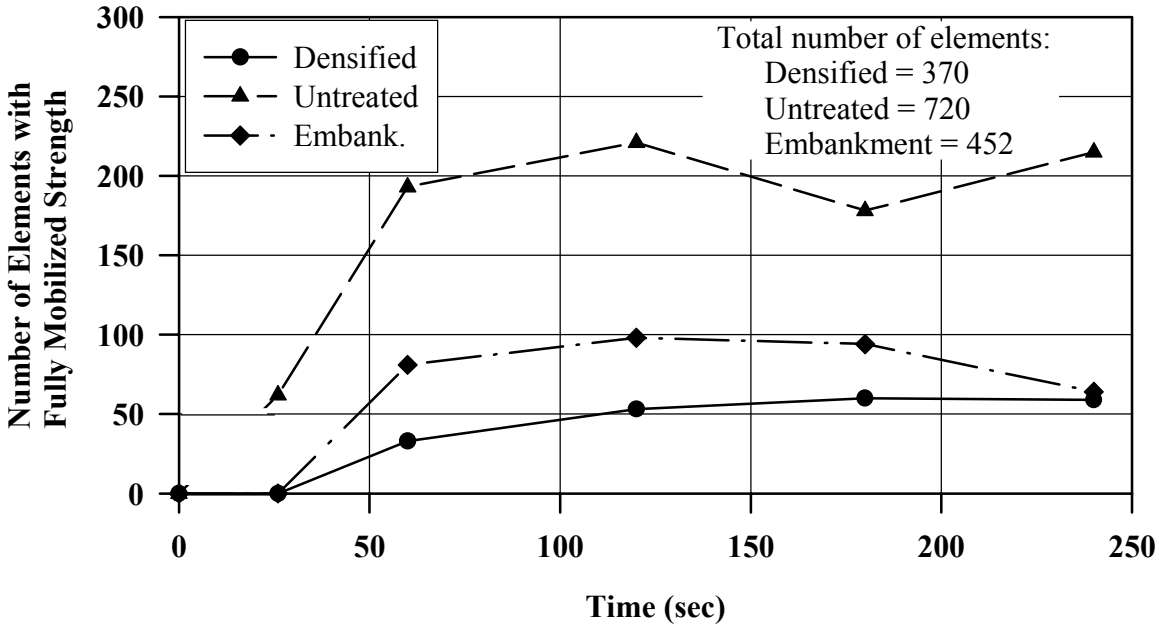

FIGURE 8.26: Number of Elements with Fully Mobilized Strength in Different Areas for 39-m-wide Densified Zone at Dr = 85% (Case J)

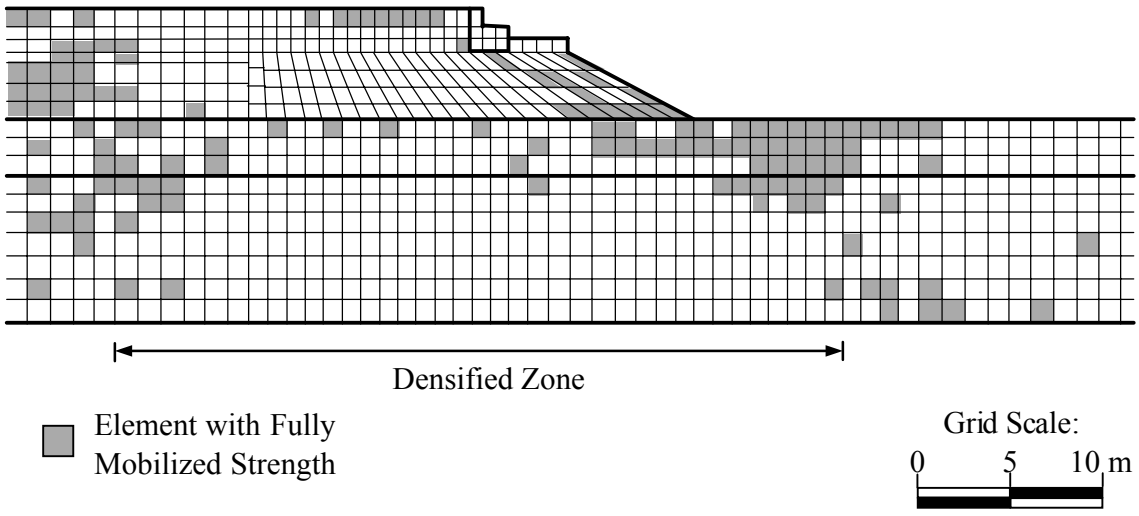

FIGURE 8.27: Pattern of Grid Elements with Fully Mobilized Strength at a Time of 180 Seconds for a 39-m-Wide Densified Zone with Dr = 85%

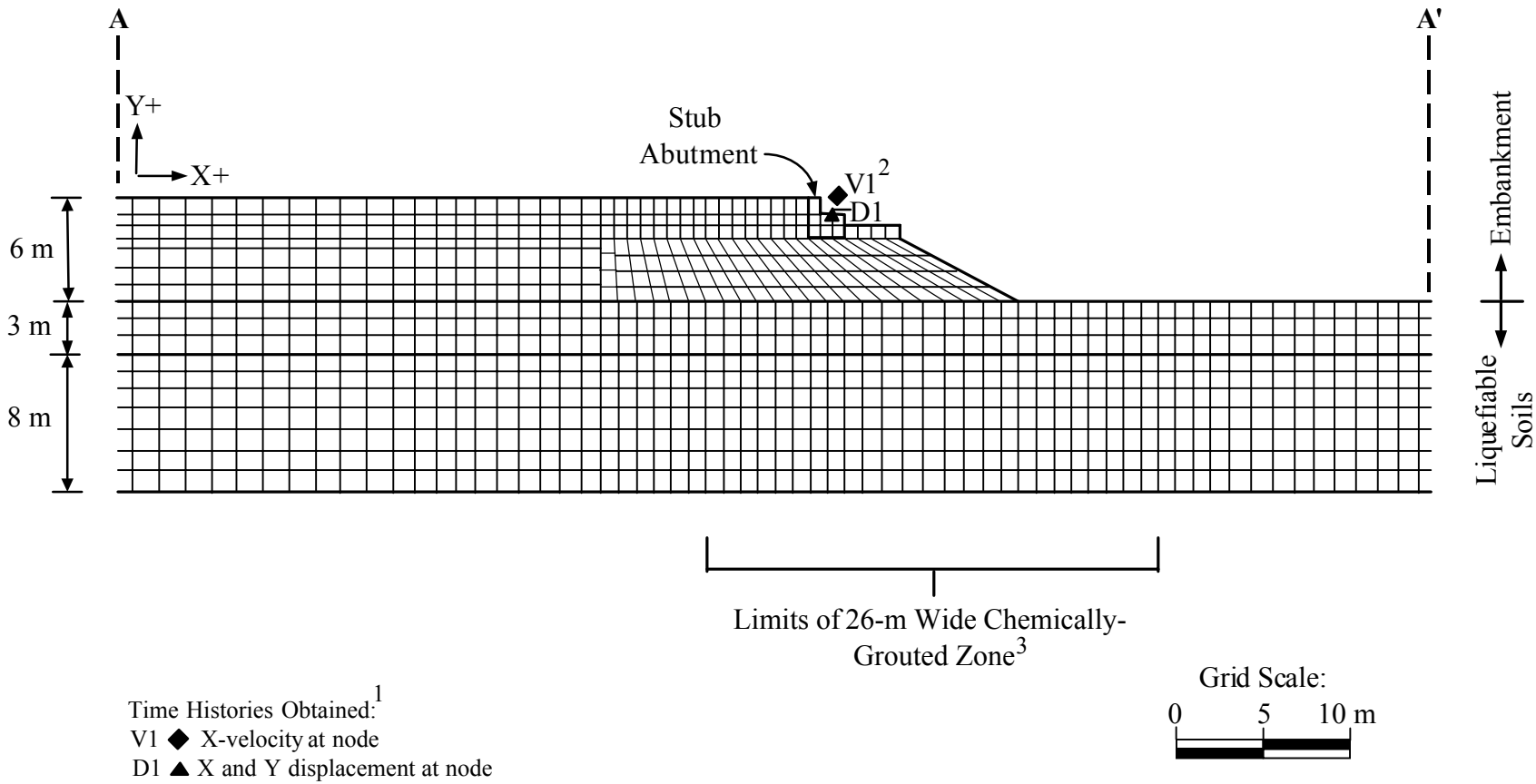

Notes: 1. Symbol indicates a predicted time history for a particular element or node is presented in a figure.
2. V1 shown offset from its actual location, which is the same place as D1.
3. Detailed results and discussion presented in text for 11-m-thick chemically-grouted zone, in liquefiable soils, having limits shown.
4. Two rows of elements representing 2-m-thick dense sand layer added to bottom of grid for analysis, but are not shown.

FIGURE 8.28: Expanded Section A-A' of Grid Used for FLAC Analysis of Stub Abutment with Chemically-Grouted Zone

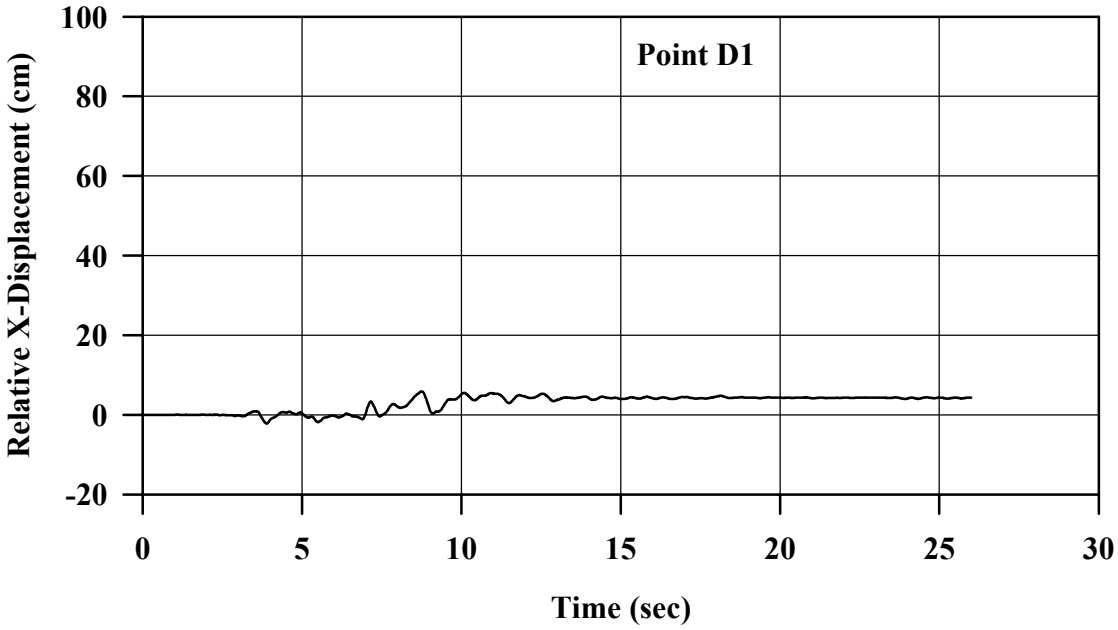

FIGURE 8.29: Relative X-Displacement Between Stub Abutment and Base of Grid vs. Time for 26-m-Wide Chemically-Grouted Zone

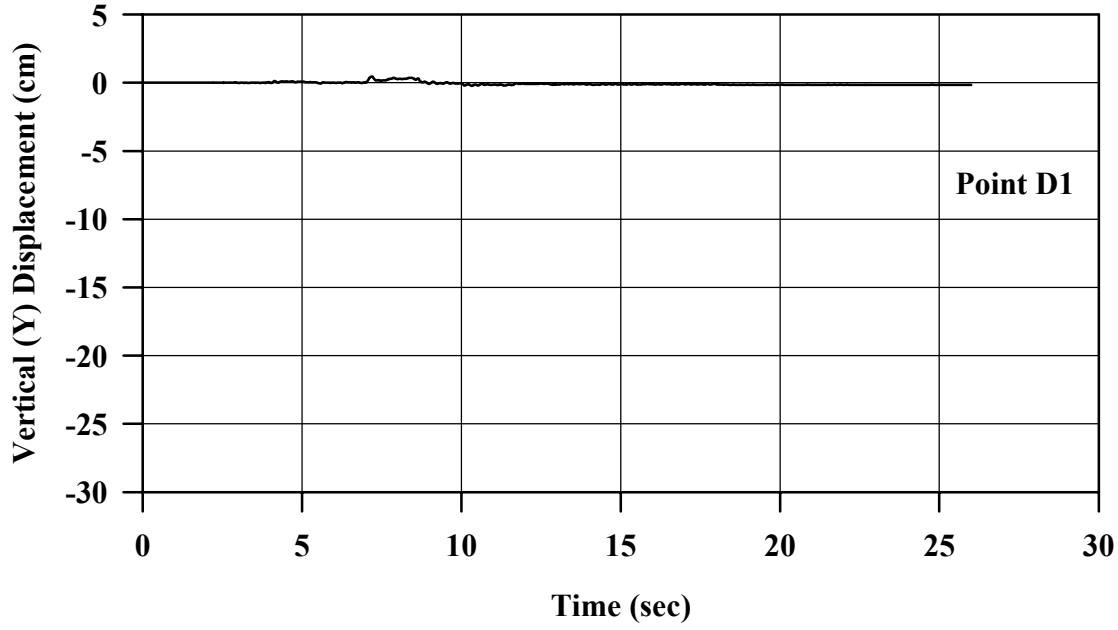

FIGURE 8.30: Vertical Displacement of Stub Abutment vs. Time for 26-m-wide Chemically-Grouted Zone

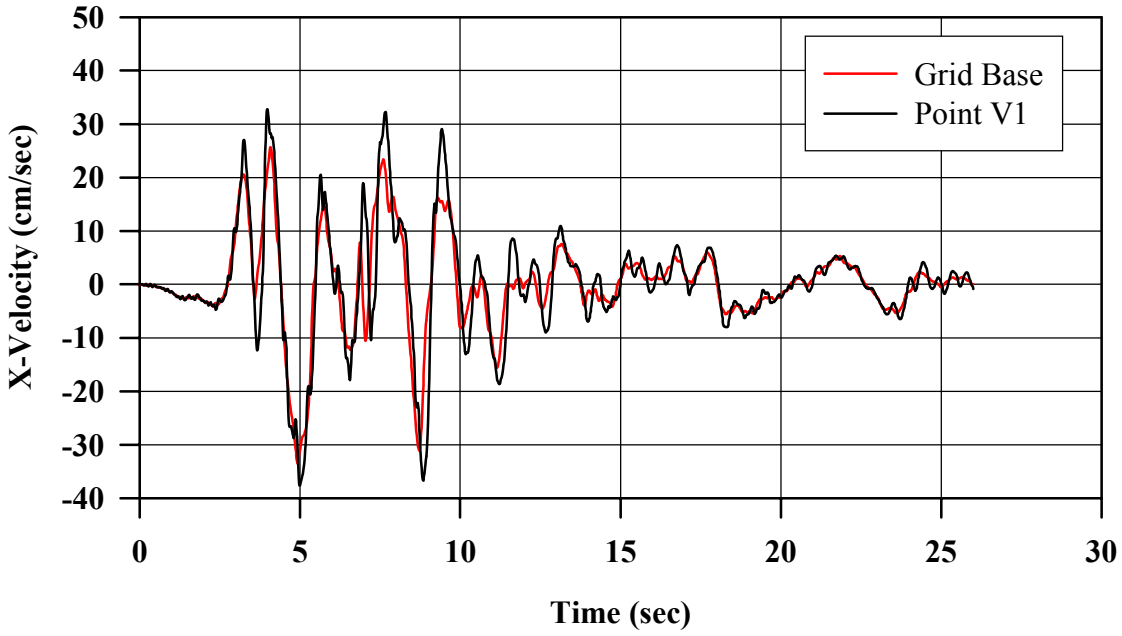

FIGURE 8.31: X-Velocity of Grid Base and Stub Abutment vs. Time for 26-m-wide Chemically-Grouted Zone

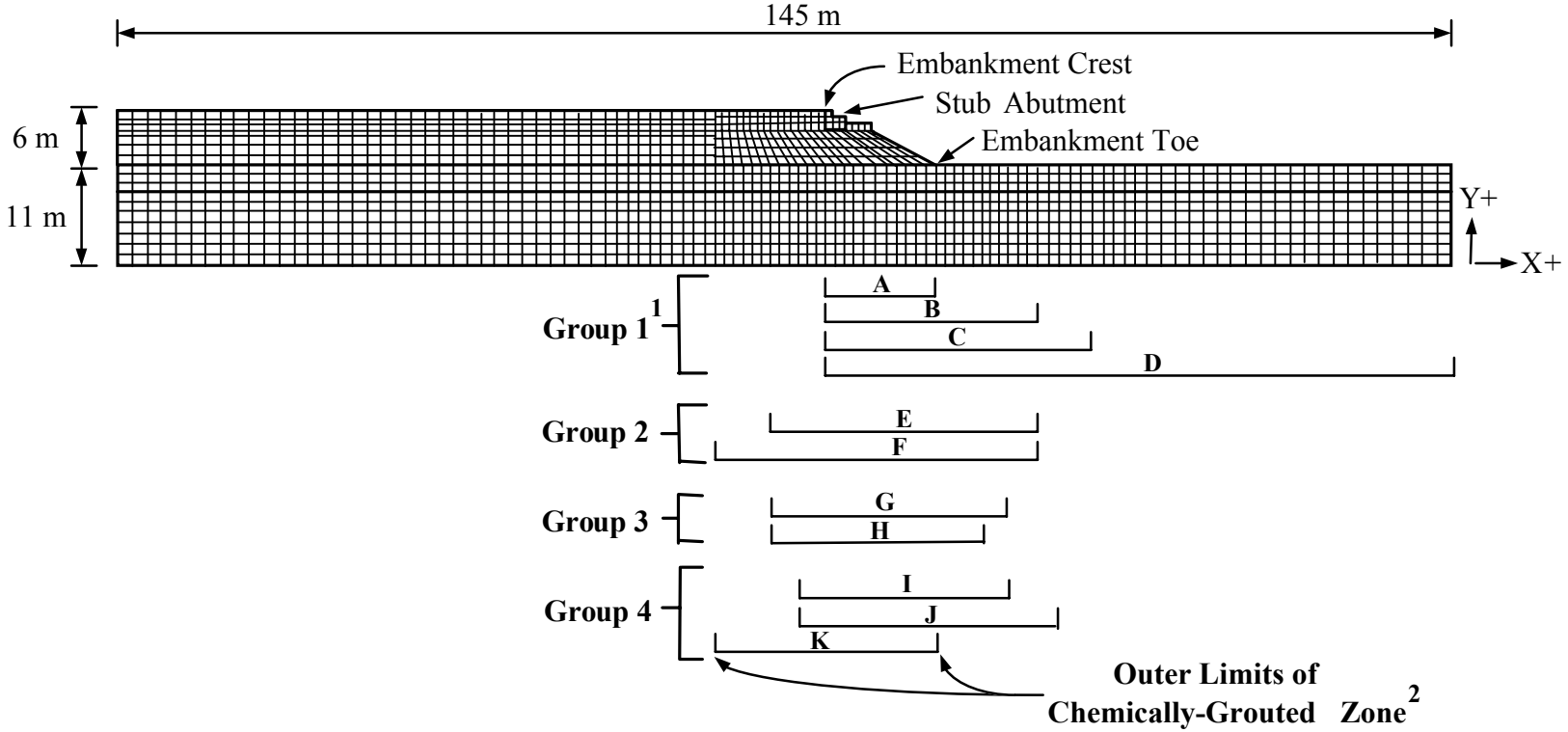

Notes: 1. Groups include analyses performed of abutment with chemically-grouted zones having different sizes and locations shown (each one is assigned a letter which is used as a reference). Details concerning zone dimensions and locations are provided in Table 8.3. All zones are 11-m-thick, extending from the bottom of embankment to bottom of liquefiable soils.

2. All sands within outer limits shown are chemically grouted.

3. Two rows of elements representing 2-m-thick dense sand layer added to bottom of grid for analysis, but are not shown.

FIGURE 8.32: Cases Evaluated in Parametric Study of Chemically-Grouted Zones at Stub Abutment

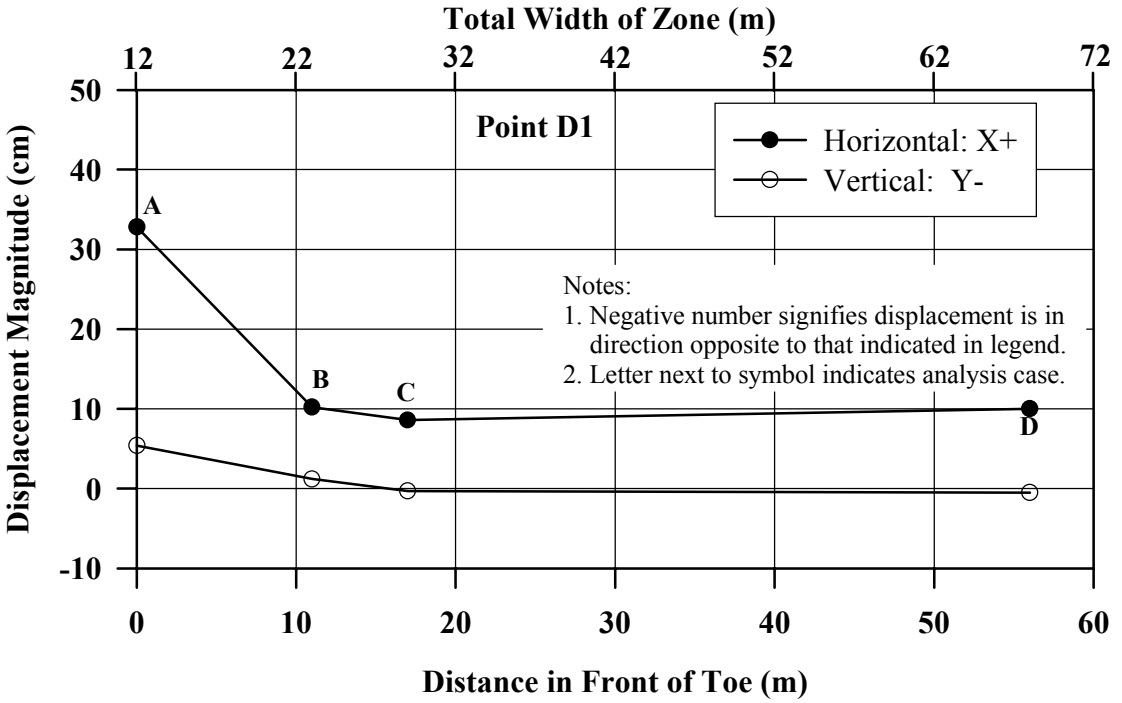

FIGURE 8.33: Displacement of Stub Abutment vs. Distance Chemically-Grouted Zone Extends in Front of Toe for Group 1 Cases

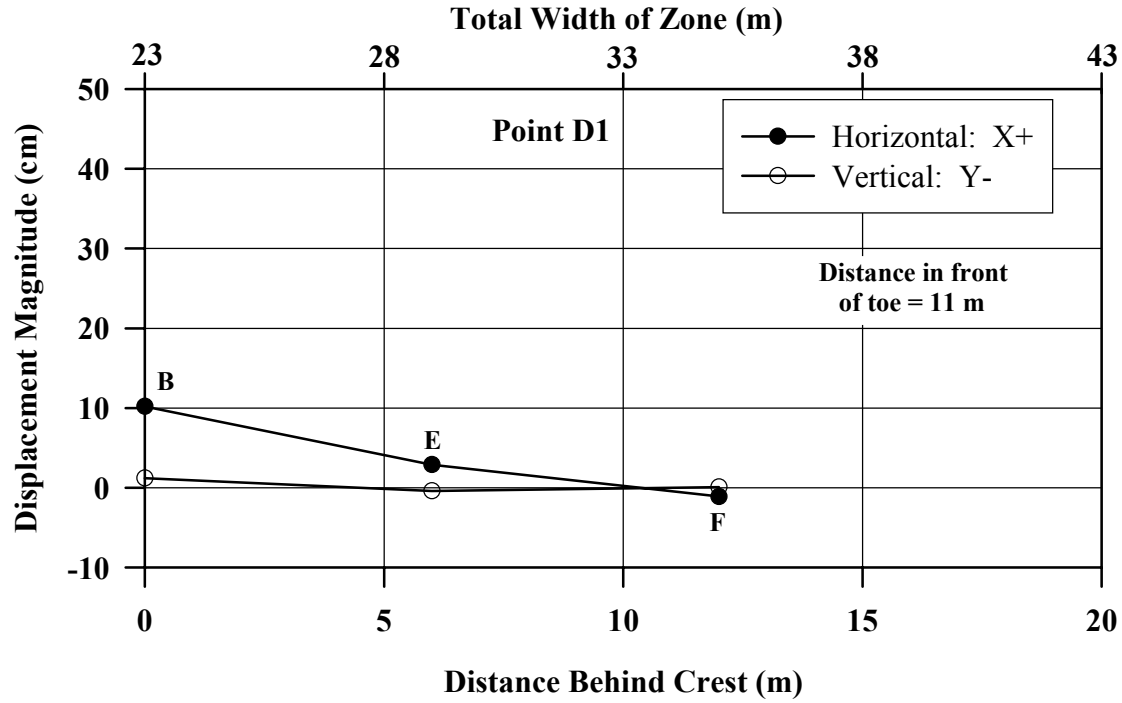

FIGURE 8.34: Displacement of Stub Abutment vs. Distance Chemically-Grouted Zone Extends Behind Crest for Group 2 Cases

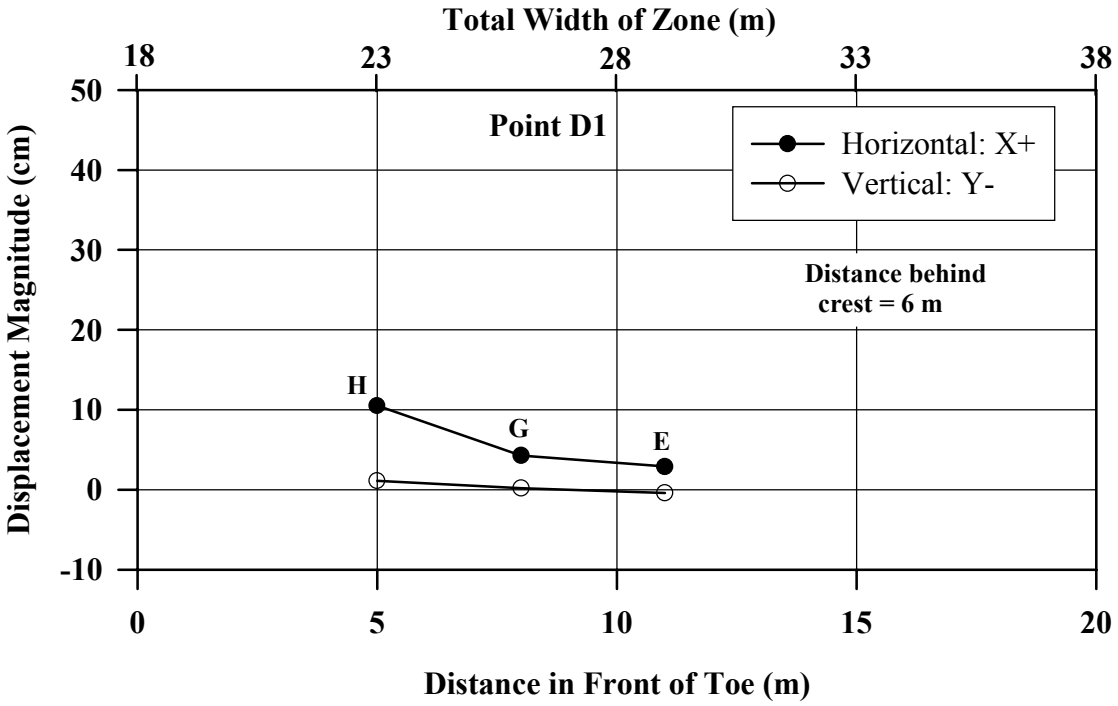

FIGURE 8.35: Displacement of Stub Abutment vs. Distance Chemically-Grouted Zone Extends in Front of Toe for Group 3 Cases

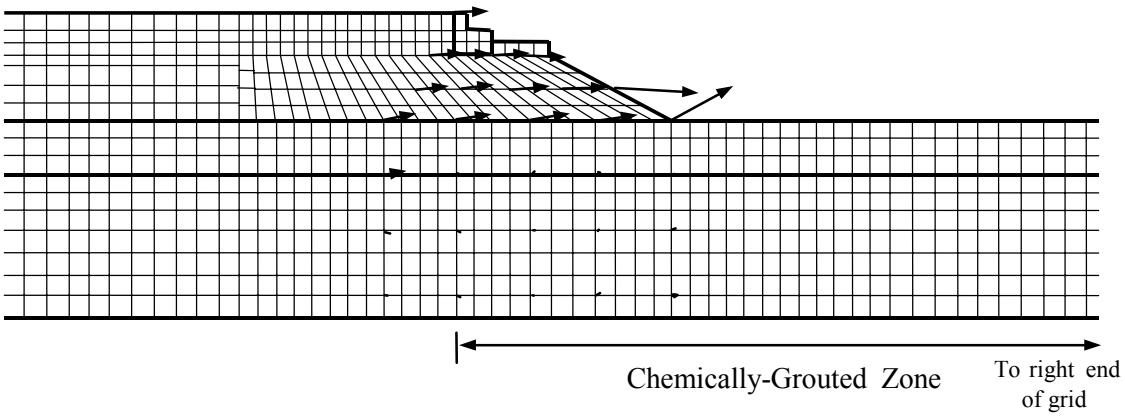

Note:
1. Displacement vector is for node located at tail of vector.
2. Bottom row of elements representing dense sand layer not shown.

Displacement Vector Scale:

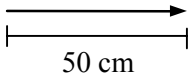

Grid Scale:

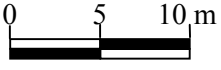

FIGURE 8.36: Displacement Pattern in Vicinity of Stub Abutment for Chemically-Grouted Zone Under Embankment Slope and Outside Embankment (Case D)

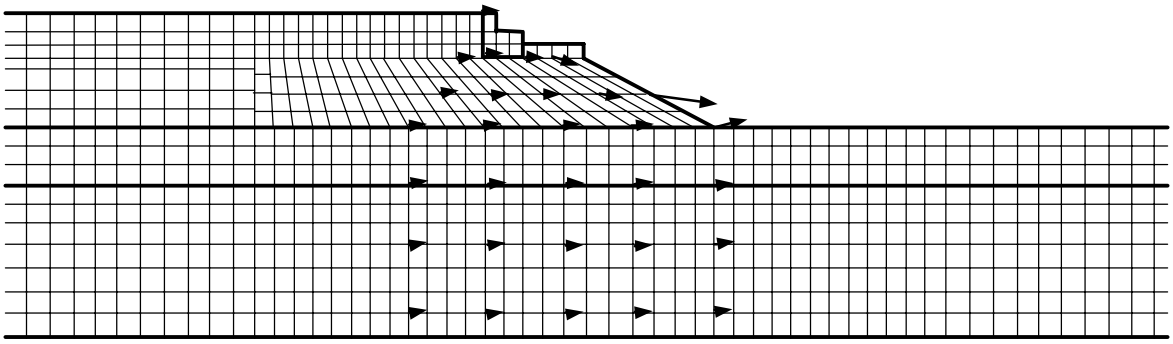

Note:
1. Displacement vector is for node located at tail of vector.
2. Bottom row of elements representing dense sand layer not shown.

Displacement Vector Scale:

50 cm

Grid Scale:

0 5 10 m

FIGURE 8.37: Displacement Pattern in Vicinity of Stub Abutment for 26-m-wide Chemically Grouted Zone Starting 6 m Behind Embankment Crest (Case G)

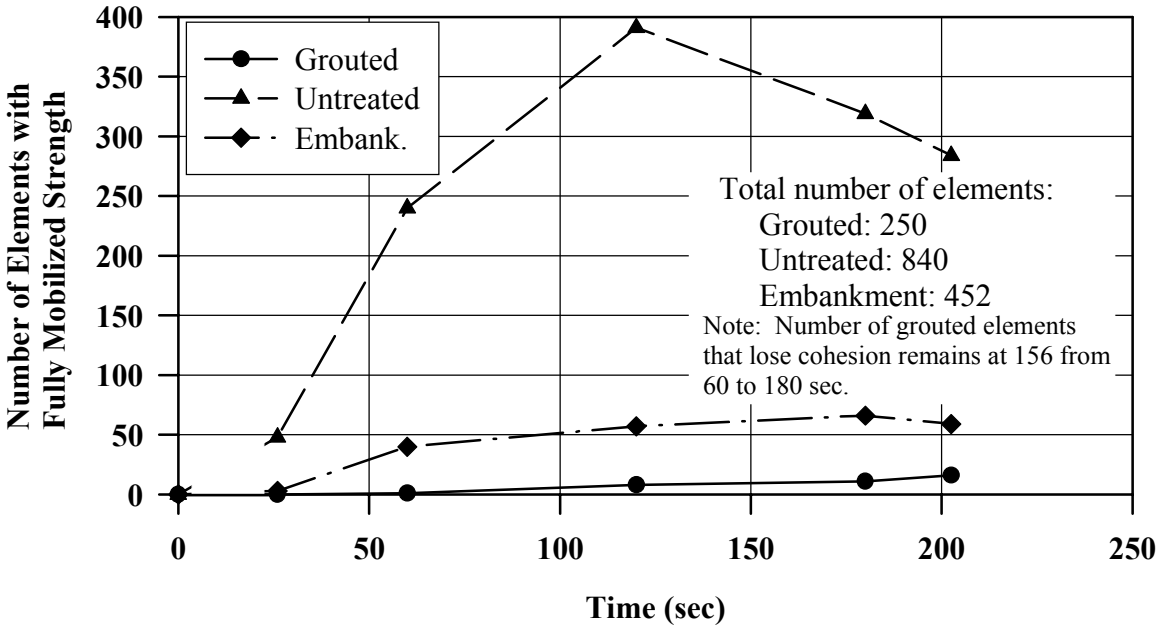

FIGURE 8.38: Number of Elements with Fully Mobilized Strength in Different Areas for 26-m-wide Chemically-Grouted Zone (Case G)

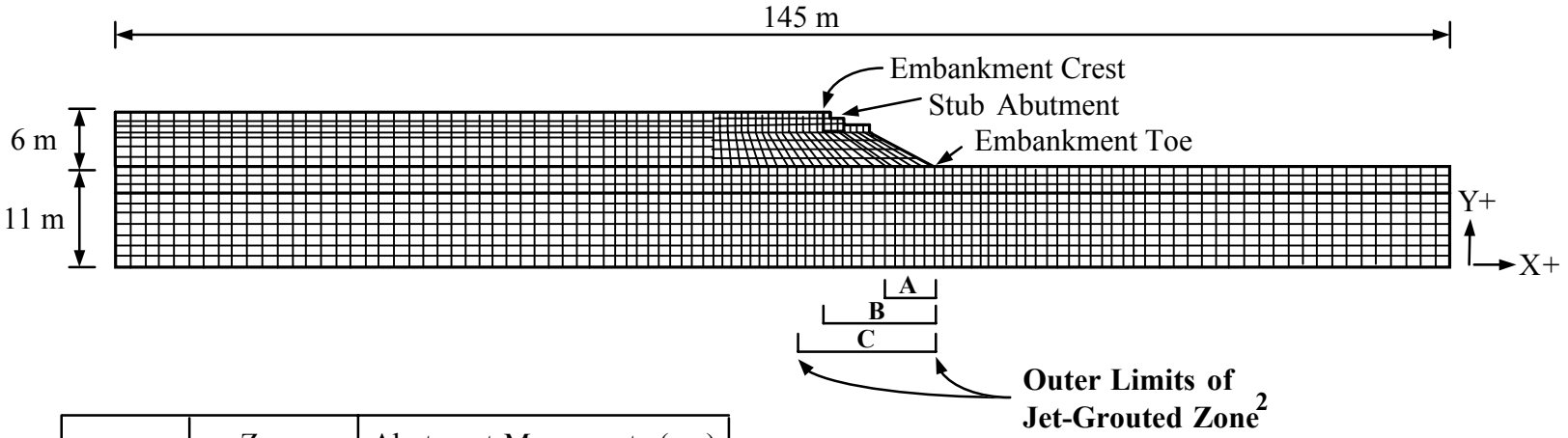

Case	Zone Width (m)	Abutment Movements (cm)	
		Vertical	Horizontal
A	5.5	-15.9	45.3
B	11	2.8	6.7
C	15	1.3	3.0

Notes: 1. Two rows of elements representing 2-m-thick dense sand layer added to bottom of grid for analyses, but are not shown. Jet-grouted zone extends downward from bottom of embankment and penetrates 1 meter into this dense sand layer.

2. All sands within outer limits shown are jet-grouted. Letter refers to particular case analyzed. For each case the width of the treated zone and predicted horizontal and vertical movements of abutment at Point D1 are provided in above table.

FIGURE 8.39: Cases Evaluated in Parametric Study of Jet-Grouted Zone at Stub Abutment

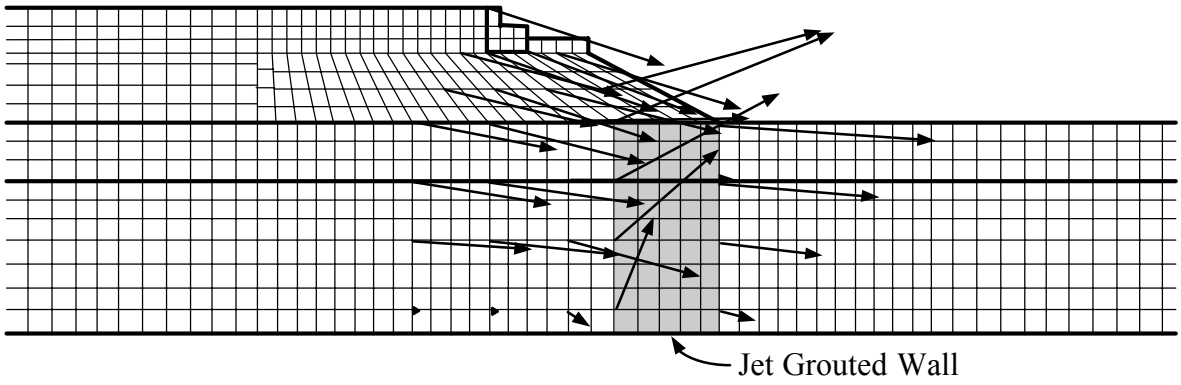

Note:

1. Displacement vector is for node located at tail of vector.
2. Bottom two rows of elements representing dense sand layer not shown.

Displacement Vector Scale:

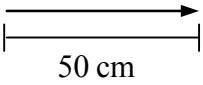

Grid Scale:

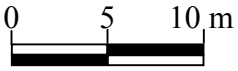

FIGURE 8.40: Displacement Pattern in Vicinity of Stub Abutment for 5.5-m-wide Jet-Grouted Wall

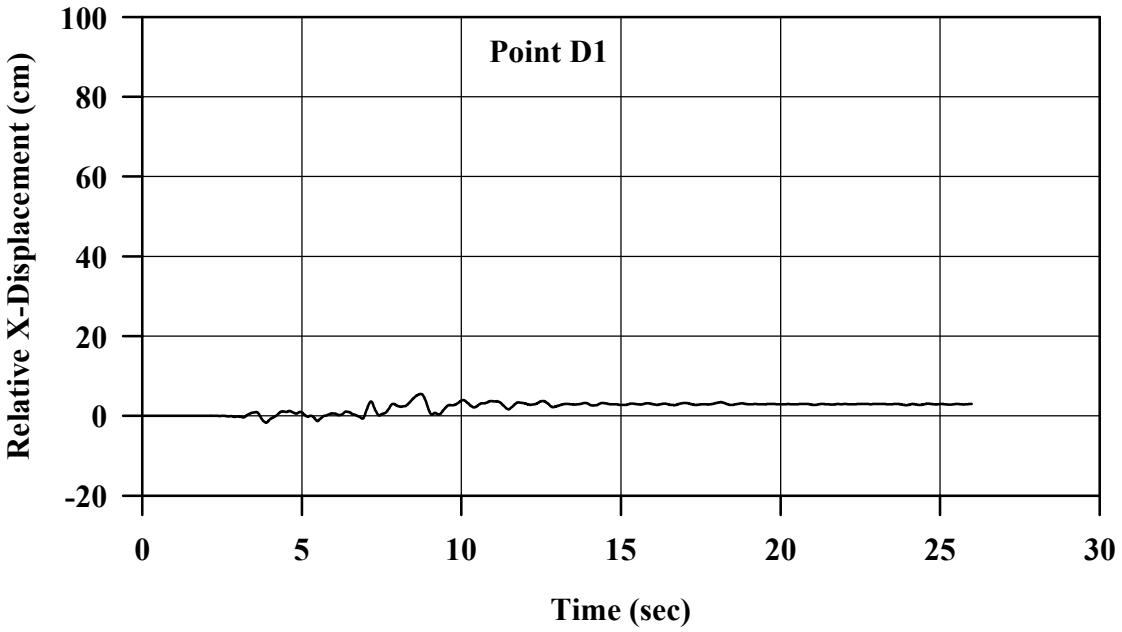

FIGURE 8.41: Relative X-Displacement Between Stub Abutment and Base of Grid vs. Time for 15-m-wide Jet-Grouted zone

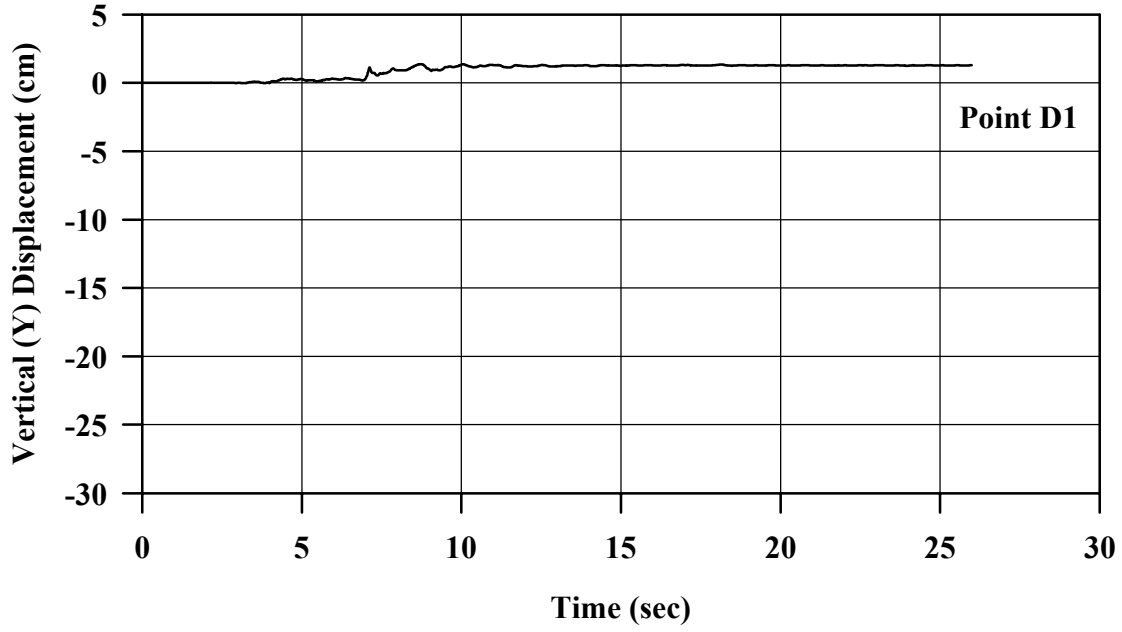

FIGURE 8.42: Vertical Displacement of Stub Abutment vs. Time for 15-m-wide Jet Grouted Zone

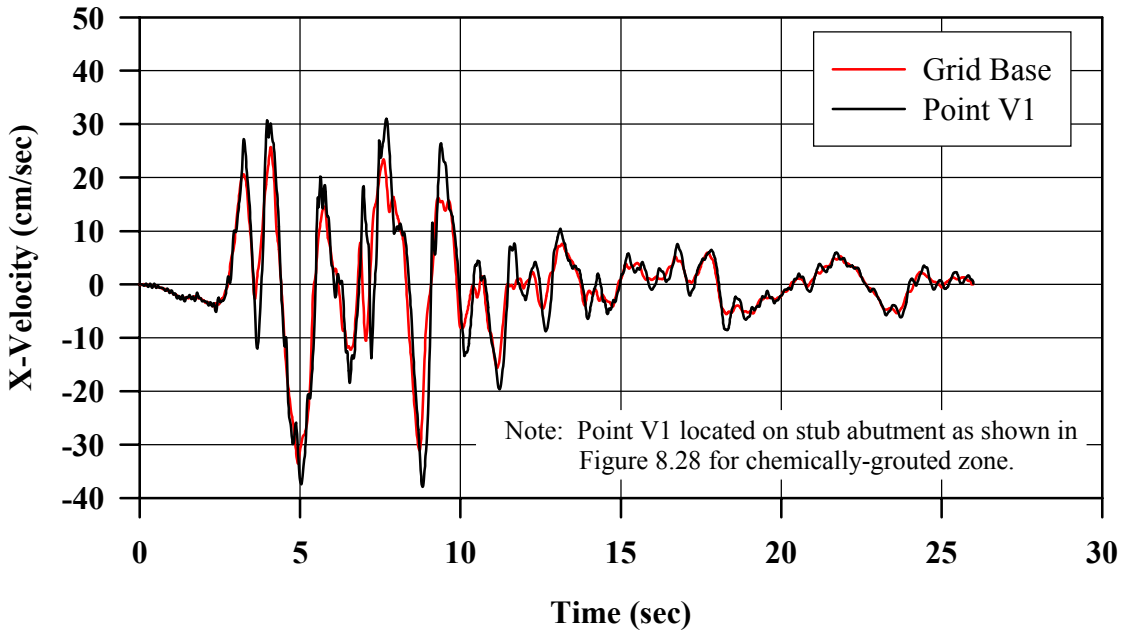

FIGURE 8.43: X-Velocity of Grid Base and Stub Abutment vs. Time for 15-m-Wide Jet-Grouted Zone

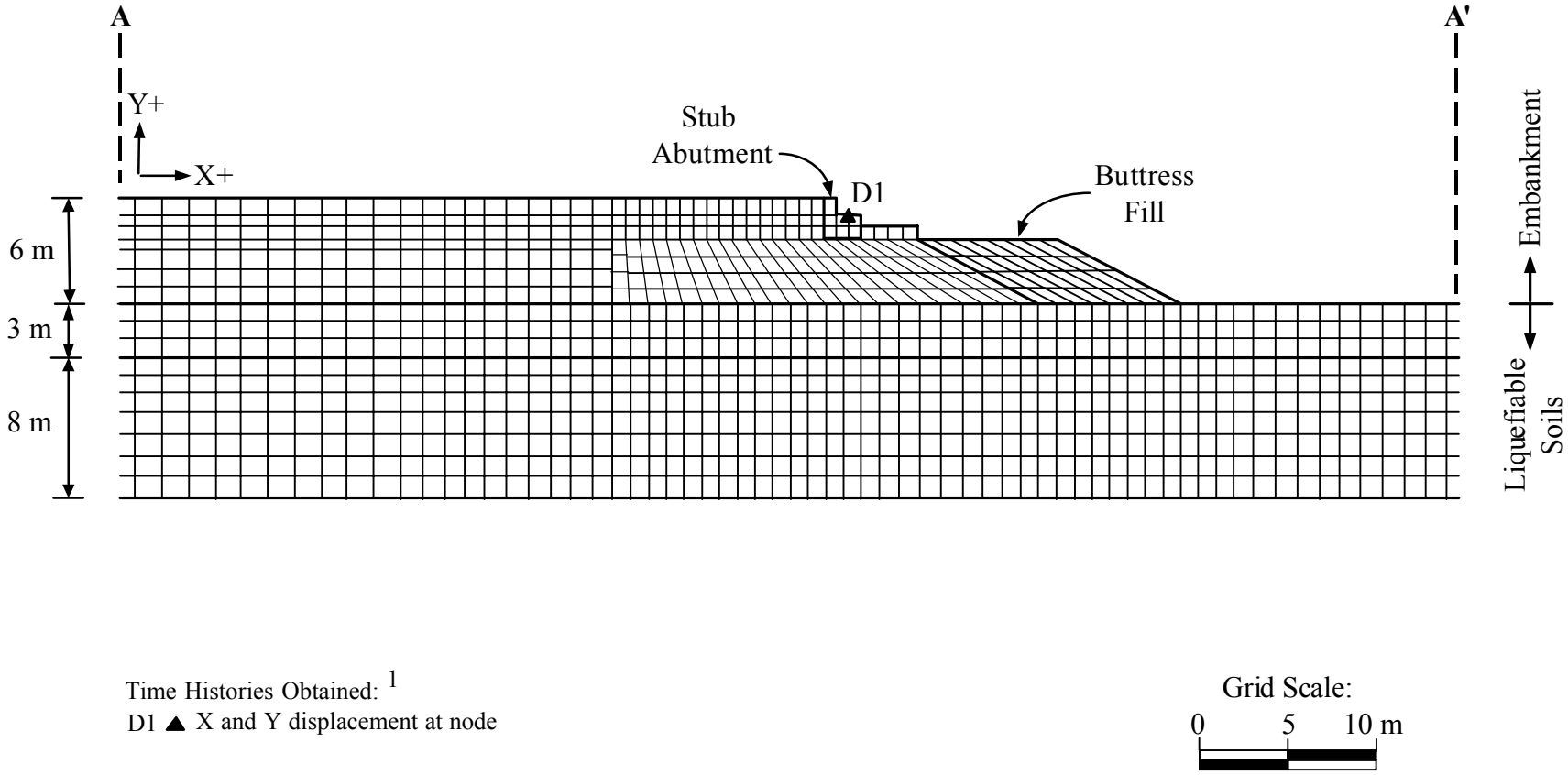

Notes: 1. Symbol indicates a predicted time history for a particular element or node is presented in a figure.

FIGURE 8.44: Expanded Section of Grid Used for FLAC Analysis of Stub Abutment with Buttress Fill Placed Against Embankment Slope

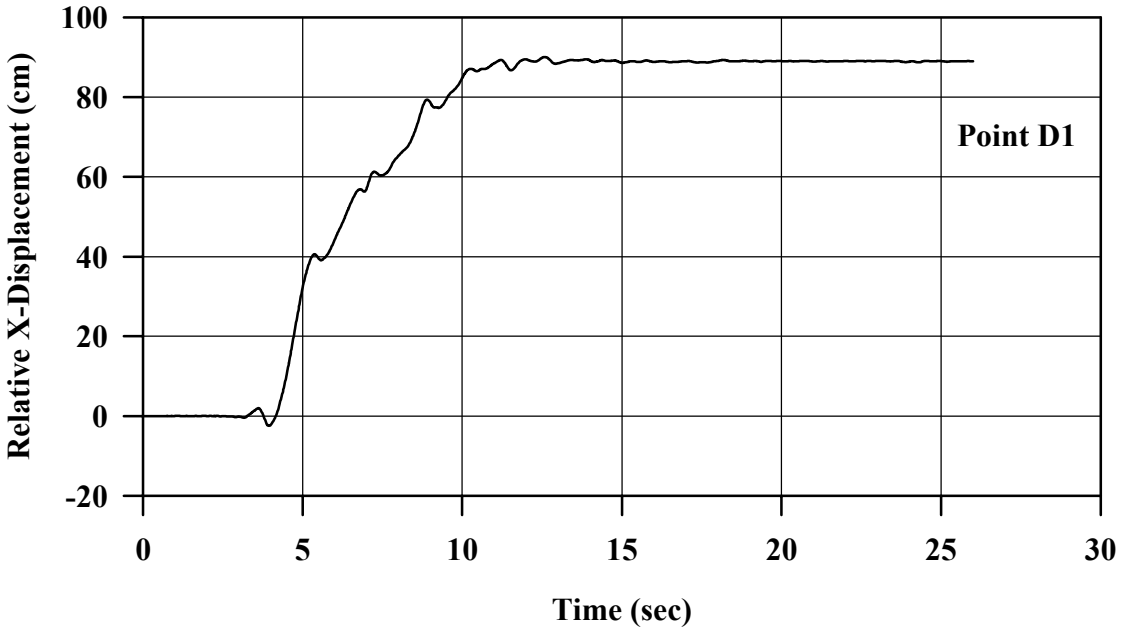

FIGURE 8.45: Relative X-Displacement Between Stub Abutment and Base of Grid vs. Time for Buttress Fill

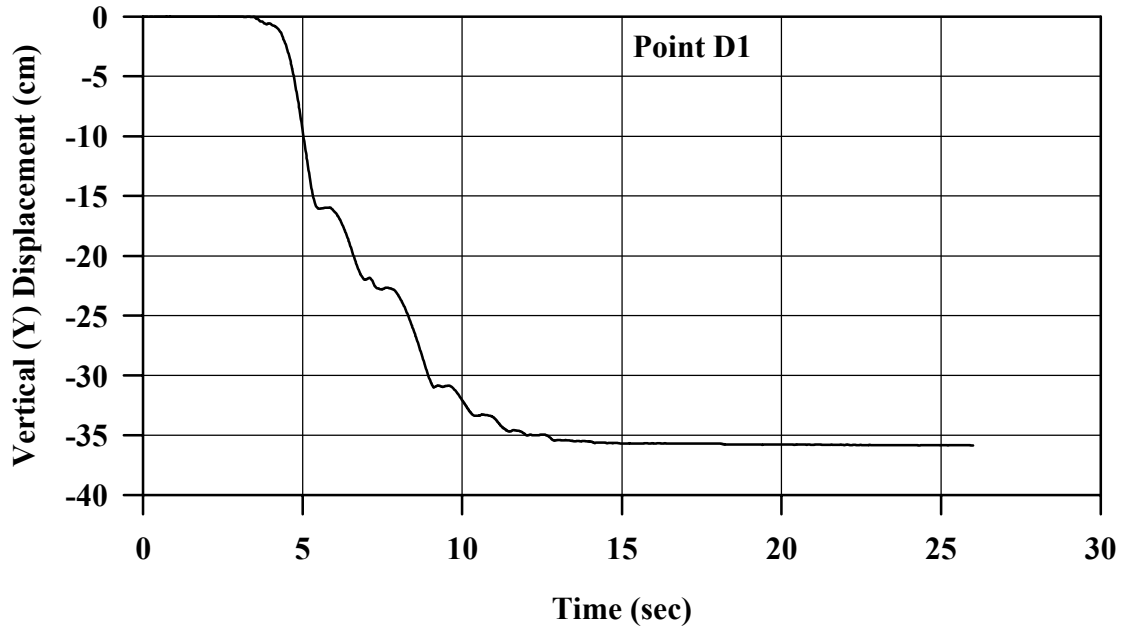

FIGURE 8.46: Vertical Displacement of Stub Abutment vs. Time for Buttress Fill